Submission of coursework for Physics and Astronomy course PHASM201/PHAS3400

Please sign, date and return this form with your coursework by the **specified deadline** to the Departmental Office.

DECLARATION OF OWNERSHIP

- I confirm that I have read and understood the guidelines on plagiarism, that I understand the meaning of plagiarism and that I may be penalised for submitting work that has been plagiarised.
- I confirm that all work will also be submitted electronically and that this can be checked using the JISC detection service, Turnitin®.
- I understand that the work cannot be assessed unless both hard copy and electronic versions of the work are handed in.
- I declare that all material presented in the accompanying work is entirely my own work except where explicitly and individually indicated and that all sources used in its preparation and all quotations are clearly cited.

Should this statement prove to be untrue, I recognise the right of the Board of Examiners to recommend what action should be taken in line with UCL's regulations.

Signed CGomm

Print Name Christopher James Gomm

Dated 02/04/2014

Title	Date Received	Examiner	Examiner's signature	MARK

A Study Into The Liquid–Liquid Phase Separations In Binary Liquid Systems

Christopher J Gomm

Supervisor:
Professor Ian Robinson

April 1, 2014

University College London

Before this report starts I would like to quickly thank the various people who made the work that I accomplished possible. Without their help and guidance I would not have been able to complete this project:

Firstly, a special thanks Prof. Ian Robinson for helping me through the many problems that I encountered and in providing me with advise and guidance throughout this project. A big thank you to Neha Parmar for her help with risk assessments, organising my visits, my induction programmes and in teaching me the basics of practical chemistry. Without your help I still wouldn't know how to use a pipette! I would also like to thank Dr Mohammed Yusuf for helping me out with synthesis methods and for making sure my visits to Harwell were always enjoyable. Finally I would like to thank Deep for her invaluable help in using the confocal microscope and to everyone else in the research group who not only helped me with problems but also offered incredible hospitality and kindness on every visit.

Abstract

This project was designed with the main aim of locating and imaging a liquid–liquid phase boundary of a binary liquid. The liquid system was a protein–salt mixture of lysozyme & 7% w/v NaCl in a sodium acetate buffer solution of 0.1M concentration. A working synthesis method was developed and a heating method was devised based on the use of a Peltier heater. In order to image the phase changes a script was developed for the confocal microscope to take single slice images and to record intensities at single depths. This was then used to investigate how the intensity changes in depth for solutions that went through a change in phase. In the clear phase light was able to pass an extra 6–8μm through the sample compared to the cloudy phase before the intensity dropped off. Investigations also found the cloud point temperatures for various lysozyme concentrations (in a 7% w/v NaCl, 0.1M, pH 5.2 sodium acetate buffer solution): $28.65 \pm 0.35\,^{\circ}\mathrm{C}$ *(100mg/ml),* $26.35 \pm 0.45\,^{\circ}\mathrm{C}$ *(80mg/ml) and* $24.55 \pm 0.35\,^{\circ}\mathrm{C}$ *(60mg/ml). Attempts were made to image the fluctuations in phase on the cloudy phase boundary of the solutions. However problems with the control of the environment around the samples and with the accuracy of the temperature control led to unsuccessful results. As a result various improvements to the experiments were suggested including an "oven within an oven" for heating and the use of a thin rectangular capillary for better isolation of the samples.*

Contents

1 Introduction **5**

1.1 Aims, Objectives and Motivation 5

1.2 Theory 9

1.2.1 Choosing The Binary Liquid 9

1.2.2 Understanding Phase Changes 11

1.2.3 Literature Review of Lysozyme–Salt Mixtures 15

2 Experimental Equipment and Techniques **21**

2.1 Introduction 21

2.2 Confocal Imaging 22

2.3 Stage and Heating Method 25

2.4 Synthesis of Lysozyme–NaCl Mixture 30

3 Results **33**

3.1 Initial Experimentation 33

3.1.1 Introduction 33

3.1.2 Crystal Imaging Using Continuous Scanning Method 34

3.2 Imaging The Cloudy Phase Boundary 37

3.2.1 Introduction 37

3.2.2 Effect Of Temperature On The Intensities Of The Slices . . 37

3.2.3 Adjusting Temperature to Locate The Phase Boundary . . . 45

3.2.4 Imaging Fluctuations On The Phase Boundary 50

4 Suggested Improvements To Methodology **53**

5 Conclusion **55**

6 Appendix **62**

6.1 Heating System – Temperature Dependence Graphs 63

6.2 Script Files 66

6.2.1 Z–Stacking Script 66

6.2.2 VBA .csv Importing Script 69
6.2.3 Intensity vs Slice Number Graphing Codes 74
6.2.4 Fitting to Experimental Values Graphing Codes 77
6.3 Experimental Images and Data 81
6.3.1 Initial Experimentation – Images and Data 81
6.3.2 Final Experimentation – Images and Data 88

1 Introduction

A phase change is defined as an abrupt change in a materials constitution into a new state that shares stable physical and chemical characteristics. The new state that the material changes into has different properties to the first state which can include changes in heat capacity, viscosity, bonding, structure, etc. This phase change is brought about through changing variables such as temperature, pressure and humidity. A simple example is that of liquid water changing to form ice when the system changes temperature through 0 °C. The case looked at in this report is of a change in phase associated with a binary liquid – that is to say a system containing two liquids. The same definition of a phase change holds for the binary liquid case, however a new variable – the relative concentration of each liquid, can also influence the phase changing behaviour of the system.

This project aims to look into not only the stable regions of a phase but also into the unstable fluctuating region between two phases. This region is known as the phase boundary and describes the point at which the liquid is on the cusp of a change in phase. On this boundary there are many exciting effects that occur including fluctuations in concentration, shape, size, heat capacity, refractive index and many more critical changes in properties caused by the changing of phases. This report will investigate the phase behaviour of lysozyme–NaCl (protein–salt) systems; more specifically it will explore the cloudy and clear phases of the system and the boundary between them.

1.1 Aims, Objectives and Motivation

The main aim of this project was to investigate the fluctuations in the properties of a binary liquid as it approaches a liquid–liquid phase boundary. For this investigation, a combination of confocal and ptychographic imaging techniques were to be used to develop images and acquire data regarding the phase changing dynamics on this boundary.

Objectively, the first step was finding a system where this phase changing behaviour was present and suitable for the experimental techniques and equipment available. In order for a successful experiment there were many restraints placed on the properties of the system. These were due to the limiting capabilities of the imaging techniques, the equipment available and also the health and safety concerns regarding the synthesis and testing of the samples. Once a suitable system was chosen the synthesis procedure and experimental setup were created, tested and refined and the necessary risk assessments and health and safety training were completed. To ensure suitability of the experimental method and imaging methods, calibration and basic testing was then performed. This testing also helped with learning how to use the equipment and gave initial indications of the response of the liquid when changes were made to variables such as temperature and concentration.

With the initial testing completed the next step was to investigate the phase behaviour of the binary liquid using the confocal imaging equipment. Initial experimentation looked into how the phase change affected the transmission of light through the liquid. Also there was some experimentation investigating some of the other properties of the liquid e.g. crystal formation and the effects that the different synthesis methods had on the dynamics of the system. The phase boundaries were then located and by holding the liquid on one of the phase boundaries, a confocal microscope was used to image the resulting fluctuations and mixing of phases. Part of the planning was for this experimentation to be expanded to involve the use of ptychography for imaging. This method would enable the gathering of more information regarding the fluctuations in phase, as this technique has a unique ability to probe the phase shifts caused by the mixing of the different refractive indexes on the phase boundary. This ability would enable the imaging of previously unseen characteristics of the mixing liquid such as how the refractive index changes over a phase change. Owing to the limited research into imaging

liquid phase changes using ptychography, this approach would also aid the development of the imaging process.

The type of binary liquid solution finally chosen was a protein–salt mixture (specifically lysozyme–NaCl). This was chosen both through its suitability to the experimental limitations and also through the fact that these results would have an impact in many other exciting areas of research. This far reaching influence includes many biological and medical applications as well as helping to solve drug delivery problems and the control of protein crystal growth in x–ray diffraction experiments.

In protein–salt systems the phase change that is of greatest importance is the one that causes the protein solutions to change from a clear phase into a cloudy phase. The cloudy phase (named after its cloudy appearance) consists of a mixture of protein rich and protein poor phases. The clear phase does not exhibit this mixing of phases and contains only a singular concentration of protein. This phase change plays an important step in the causing of sickle cell anaemia [1], cryoimmunoglobulinemia [2] and plaque formation in Alzheimer's disease [3]. It also plays a significant role in cataract formation whereby the change in phase of a protein solution causes cloudy patches to form which impair vision (cataracts) [4]. In all of these examples, the understanding of the phase behaviour of protein–salt solutions could potentially provide solutions for their treatment and prevention.

Another field of research that benefits significantly from these investigations is crystallography. This field of study involves the studying of crystal structures (including protein crystals) through single crystal x–ray and neutron scattering experiments. The success of this diffraction imaging technique is heavily dependent on the quality of the crystal; where properties such as the size, the isotropic quality and the structure of the crystals greatly affect the quality of the data obtained. When investigating protein structures, protein–salt solutions are often

used to create the crystal samples. In order to form samples with the required crystal properties the liquid solution must be held at the correct incubation conditions (defined by the phase behaviour of the liquid system). By investigating the phase behaviour of protein–salt solutions, these crystal properties can be predicted and controlled and help to ensure successful crystal formation. Such knowledge allows experimentalists to create the crystal samples required for analysis without having to use lengthy and costly trial and error methods to create the required samples [5]. With the correct samples created, these scattering techniques can be used to obtain the precise atomistic structure of the proteins in the crystal; a piece of information that is absolutely invaluable in drug design and disease treatment.

Other areas of interest include its applications to drug delivery [6, 7] and in purification of protein products [8].

Additionally the imaging of the phase boundary behaviour is relatively unexplored and is not something that has been achieved before in protein–salt solutions using confocal or ptychographic imaging. In fact the use of ptychography in imaging phase changes has not been achieved before in any system, so to be able to perform this presents an exciting challenge. Typically the majority of research into the protein–salt behaviour is focused around the crystal formation and growth; as a result there isn't much research or literature surrounding the phase boundary behaviour of these liquid systems. This project presents a unique angle for research which coupled with the numerous applications associated with this research, provides strong motivations for the completion of this report.

1.2 Theory

1.2.1 Choosing The Binary Liquid

In order to investigate a binary liquid using the proposed imaging methods a set of criteria was made to judge potential binary liquid systems against their suitability with the experimental procedures that were to be used. These criteria included temperature limitations, the length scale of the phase changes, the refractive index differences between phases and health and safety concerns.

The chosen binary liquid system must undergo a phase change within achievable temperature limits of 0 °C and 70 °C. This range was chosen to reduce the chance of condensation on the imaged surfaces and convection currents within the sample. When water condenses onto the glass slide/microscope lens the accuracy of the imaging is reduced as light travelling through these droplets may cause distortion effects in the image. These are mostly caused by refraction and reflections of the light as it passes through the droplet which can cause different phase contrasts when using phase contrast imaging equipment such as ptychography. These lensing effects also cause problems when imaging using confocal microscopy as they lead to distortions and intensity spikes in the images. Convection currents were an unwanted effect due to the mixing effects that occur when convection currents form. This would mean that the sample would not be at uniform temperature and may influence the mixing of the phases near to the phase boundary. These effects, however small, may have a large impact on the system as binary liquids have a very sensitive response to changes in temperature. These effects can be reduced by heating slowly and using a temperature range that does not encourage convection currents. Additionally using large limits in the temperature range could affect the working limits of the components used in the experiment. For example, when using a more extreme range, the magnification lenses used in the confocal imaging equipment are more prone to damage and failure.

The liquid must also have a significant refractive index difference between

phases in order for the ptychography setup to be able to measure the changes in phase distinctly.

As well as these, the changes in phase must have a length scale between 1μm and 500μm in order for the phases to be resolved when using confocal and ptychography based imaging techniques. This is due to the magnification limits of the imaging techniques. The magnification lenses on the confocal equipment and the power of the illuminating light source used in the ptychography setup determine the accuracy of the imaging methods at very high resolutions. Typically, when imaging phase changes that have length scales lower than 1μm, the imaging techniques will not be able to resolve the small fluctuations in phase change. In this project, the confocal microscope has lenses that can achieve this range through the use of the maximum magnification lens (100x) and the ptychography setup uses a 4mW, 406nm LASER which is capable of a similar resolution. It should be noted that there is also a large length scale limit that is placed onto the system, which is due to the limitations in the heating method. The heating method may not be able to provide exactly uniform heating throughout the imaged area and with large scale phases there is a higher chance that there will be a temperature gradient large enough in the field of view that causes visible differences in the behaviour of the phases being imaged.

The final and more trivial of the conditions was that the solution had to be relatively safe and non–hazardous. This was mostly to help increase the chances of the experiment passing strict risk assessment procedures and health and safety requirements in the lab. It would also help speed up the time taken for the risk assessment to be reviewed and accepted.

These conditions narrowed down the choice of potential binary systems to only a handful of choices. The two binary liquids that were short–listed for experimental testing were a lysozyme and salt mixture and a triethylamine (TEA) and stearic

acid mixture. These both met with the criteria required however, it was decided that the lysozyme–salt system would be the focus for this project. The reasons behind this decision included: an easier synthesis procedure, more interesting behaviour (including crystal formation) and also that the influence of research into lysozyme–salt solutions is more extensive and that the results will have more interesting applications (including those within the medical profession and x–ray crystallography experiments). There are numerous salt types that could have been used for this investigation, but in this project only the use of NaCl was looked at, further explanation for this decision is discussed later in this section.

1.2.2 Understanding Phase Changes

Many theories have been put forward regarding the understanding of phase changes in binary liquids. The focus on protein–salt mixing has itself been at the centre of much research due to its wide reaching impact and its influence in many medical conditions. The theoretical models help to gain a greater understanding of liquid behaviour and due to the seemingly indefinite number of binary liquid systems, the impact of such research has a influence in multiple far reaching fields of science. Some examples of the fields that are affected by the understanding of phase changes in binary liquids include the defence industry (weapons development), crystallography and healthcare/pharmaceutical research (drug development). Another example is in the petroleum industry where it is necessary to model the phase behaviour of extracted liquids to predict the response of the liquids in the wells. It is also important in the development of new fuels and in improving extraction techniques [9].

On the boundary of a phase change there are many changes in the dynamics of the system. At the critical point, there exists a coexistence curve that defines the point at which the two phases are immiscible. At this point, the liquid experiences critical behaviour and can have fluctuations in heat capacity, thermal expansion and concentration [10]. Fluctuations in concentration lead to an inhomogeneous

refractive index, which can in turn give rise to the phenomenon of critical opalescence. Other features which change within the liquid include phenomena related to the interfaces in a binary fluid. These include the critical interface (the boundary between the two coexisting phases below the transition temperature) and the semi–critical interfaces (e.g. the interfaces between the liquid and the boundary walls) [10]. Such interfaces would exist within the lysozyme–salt phase separation; a critical interface would be that of the high and low density phases and a semi–critical interface would include the boundary between the mixture and the liquids container boundaries (e.g. the glass slides used when imaging the liquid). In this experiment the focus is largely on these critical interfaces although the behaviour of the liquid at these semi–critical interfaces would also serve as an interesting experiment.

The theoretical framework into the creation of phases within protein solutions is complex and many theories have been suggested as to how the forces between protein structures interact to create this separation. Many models have been produced to try to explain this interaction with each building on the successes and failures of previous models. Unfortunately, most models only take into account how the salt concentration and type affects the cloud point temperature and for the purposes of this project, these models were not useful. This is because only the concentration of lysozyme and temperature of the solutions were variables that were tested. When considering just the affect of lysozyme concentration there are a very limited number of models and of these models none describe the same system that is tested in this project and only one describes a similar system – differing in the use of HEPES as the buffer solution instead of the sodium acetate (NaAc) that was used in this project.

This model was created by Gogelein [5] and was built around the use of a colloidal mixing model as the basis. The original colloidal mixing model was created by E. J. W. Verwey et al. [11], who looked into the attractive and repulsive

effects between colloidal particles as a function of their separation. This is also known as Derjaguin–Landau–Verwey–Overbeek (DLVO) theory of colloidal stability. Gogelein's adaptations included improvements to suit the protein system including: using a Yukawa potential to describe radial factors, fitting experimental data to the short range DVLO potentials to describe van der Waals interactions between the protein molecules, using a hard sphere model to describe the protein solutions and accounting for screened electrostatic repulsion. This model provided results for 0.2 mol/l (1.17% w/v), 0.3 mol/l (1.75% w/v), 0.4 mol/l (2.34% w/v) and 0.5 mol/l (2.92% w/v) NaCl concentrations and varying lysozyme concentrations from volume fractions of 0–0.5. This compared well with the experimental results achieved by Cardinaux et al. [12] and Gibaud [13], but caused a disagreement with experimental results at high lysozyme concentrations. It was hoped that this model would have been used to compare with the results obtained in this experiment, however by accident the salt concentration used in this experiment was different to the range used in the model. Therefore, it would not be useful for comparisons with this project or with the data from Muschol and Manno [14, 15] (who used a comparable liquid system to the one investigated in this project).

Investigations into the salt dependence on the cloud point temperature has been modelled by Wentzel and Gunton [16] who modelled the concentrations of $MgCl_2$ and NaCl and more recently by Zhang and Cremer [17] who modelled the concentrations of $NaClO_4$, NaSCN, NaI, $NaNO_3$, NaBr and NaCl. Both offered good agreement with experimental results and are suggested as models to be used if this project was to be extended to allow for investigating salt concentration and types.

In this project it was aimed that the results would be compared to theoretical models describing the protein–salt interactions. However, the unavailability of a model that describes the same system that is tested in this project has led to the analysis of results being based solely on previous experimental results. The

experimental results gained in this project were plotted onto a suitable graph comparing the cloud point with the concentrations of lysozyme tested. This data was then be compared with the data from Muschol and Manno [14, 15] who performed an almost identical experiment, using the same salt type (NaCl) and buffer solution (NaAc) (see Figures 1 & 2). This data would then be compared with the results from this project and fitted to the scaling relation for binary de–mixing (see Equation 1) using the critical exponent of $\beta = 0.325$ [18].

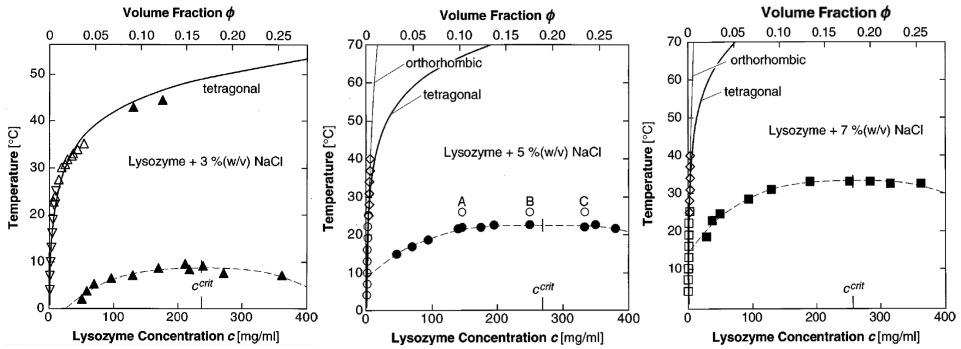

Figure 1: This diagram shows the results obtained by Muschol et al. [14]. The dashed line fits the experimental data (Solid: Triangles for 3% NaCl, Circles for 5% NaCl and Squares for 7% w/v NaCl) using Equation 1. The solid lines represent the fits to the van't Hoff equation, describing the crystal solubility temperatures for various concentrations of lysozyme.

$$T_c = T_{cr}\left\{1 - A\left|\frac{c_{cr} - c_p}{c_{cr}}\right|^{\frac{1}{\beta}}\right\} \tag{1}$$

Equation 1 is a fitting function that was used to fit the experimental data in Figures 1 & 2. T_c is the cloud point temperature, T_{cr} is the cloud point temperature for the critical concentration, c_{cr}. A is a fitting parameter and c_p is the protein concentration.

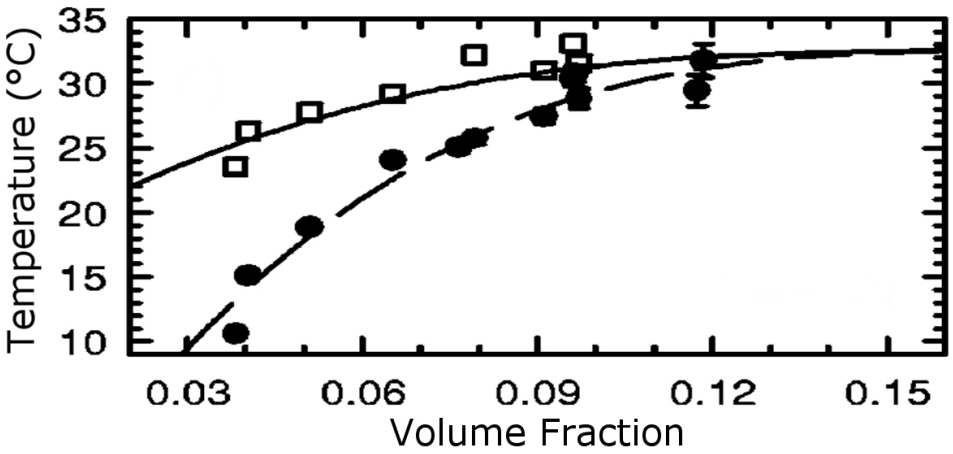

Figure 2: This diagram shows the results obtained by Manno et al. [15] where a 7% w/v NaCl and pH 4.5 NaAc buffer solution was used for concentrations of lysozyme ranging from 0–0.15 (volume fraction). The cloud point (open squares) is plotted alongside the spinodal data (circles) and is fitted using Equation 1 (the solid curve).

1.2.3 Literature Review of Lysozyme–Salt Mixtures

Lysozyme is a very common, heavily researched enzyme known mostly for its ability to break down the cell walls of bacteria and help protect from bacterial infections; properties that led it to being discovered as one of the first antibiotics. Such aqueous protein solutions crystallise and undergo a liquid–liquid phase separation under the addition of a salt such as NaCl (forming lysozyme–salt solutions). This protein crystallisation behaviour is very important in the determination of structure where techniques including: x–ray diffraction, neutron diffraction and electron microscopy, can be used to resolve the protein structure. This area of physics involving the study of crystal structures became very important in the mid–late 20th century. The first structural analysis experiments were performed in the early 1960's by D. C. Phillips [19] as a way of understanding protein structure. In fact the study into the structure of lysozyme provided the first experimental atomistic analysis of an enzymes structure and was achieved through x–ray investigations.

The crystal structures formed within these lysozyme–salt solutions experience structural changes with temperature. Between $-35\,^{\circ}\mathrm{C}$ and $25\,^{\circ}\mathrm{C}$, the crystals are tetragonal, above $25\,^{\circ}\mathrm{C}$ these crystals dissolve and orthorhombic crystals are formed [20]. There are two variations in orthorhombic structure known as low temperature orthorhombic at $25\,^{\circ}\mathrm{C}$ and high temperature orthorhombic at $37\,^{\circ}\mathrm{C}$ [21]. Both orthorhombic and tetragonal crystals are present simultaneously at $25\,^{\circ}\mathrm{C}$ but above $25\,^{\circ}\mathrm{C}$, only orthorhombic crystals are observed [20, 14].

Research by ten Wolde and Frenkel [22] showed that the critical nucleation was lowered near to the cloudy phase boundary temperature, causing an increase in the nucleation and growth rates of the crystals. This is unwanted behaviour as the crystal formation and growth affects the localised lysozyme concentrations. To compensate for this, imaging time scales must be lowered to reduce the chance of crystal formation. Examples of such crystal growth near to the phase boundary is given in the appendix (see Figure 18).

More recently, the testing of the phase behaviour of lysozyme–salt mixtures has seen a rise in publications. Most research has focused on the effects of the salt and buffer identity, the salt and lysozyme concentration and on the crystal growth dynamics when the system is subject to variable conditions such as temperature and pressure changes [14, 23, 24, 25].

The liquid–liquid phase boundary in lysozyme–salt solutions between the cloudy phase and clear phase is a very interesting phase change and is one that this project will focus on. When a concentrated lysozyme solution is cooled below the cloud point temperature it separates into two coexisting liquid phases. In this regime, pockets of a high density lysozyme phase are formed within the solution and coexist with areas of low density lysozyme concentrations. These pockets of the high density phase have a different refractive index to the less dense phase and as a

result cause a phase contrast between each phase. Research into this topic has been completed by Ball, V. and Ramsden, J. J. [23], whose research found that the refractive index of protein–salt solutions was dependent on both the salt type and the solvent (buffer) used. The research suggested that the refractive index of the solutions varied linearly with salt concentration. They also found that by changing the salt type, the linear relationship was shifted up or down in the refractive index range [23]. This research tested on NaCl and NaSCN salt types and found that the NaCl salt offered a lower refractive index difference (ranges from 0.5–0.7 depending on protein concentration) compared to the NaSCN salt (whose range was 0.55–0.9). Ideally a higher difference is wanted when using phase contrast imaging techniques like ptychography. As a result, the NaSCN salt is more suitable. However this difference is not too significant and both the refractive difference offered by NaCl and the other benefits of using a NaCl salt (to be explained in detail later in this section) outweighs this difference. No publications regarding other salts (such as NaBr, NaI, potassium based salts or divalent salt ions) were found to compare with this NaCl and NaSCN data.

The fact that there is a significant phase difference in protein–salt solutions allows the exploration of dynamics that may not be visible using traditional imaging techniques. It confirms that the use of ptychography (or any other suitable phase contrast imaging method) is suitable in this project and that by using these methods it would be possible to extract more information regarding the processes occurring in a phase change.

Research by Bostrom et al. [26] has investigated how the identity of the salt changes the phase behaviour of the solution. By using Monte Carlo simulations and fitting to experimental data they were able to produce a working model for creating phase diagrams for NaSCN, NaI and NaCl lysozyme solutions. In this model the forces between protein globules, ions in the sample and the forces between each ion and protein globule were investigated. When the interaction potential

between these combinations is sufficiently short–ranged, the stable liquid–liquid phase transition disappears and only the solid–liquid coexistence curve is thermodynamically stable. The use of different salt ions can adjust this interaction range and as a result they can alter the phase change behaviour of the solution. The use of NaCl as the salt in the lysozyme mixtures lead to lysozyme–lysozyme protein attractions of a larger strength compared to NaI and NaSCN salts. Their findings suggested that the use of NaCl as the salt created stable liquid–liquid phase separations, whereas the use of NaSCN could not support a stable separation (thus ruling NaSCN out). The temperature range of the transitions also occurred around approximately 25 °C for the NaCl solutions. This is beneficial for the interests of this study as this temperature range is easily accessible using inexpensive heating methods, a property which factored into the decision for NaCl to be used in this project.

Research by Huang et al. [27] also found how the salt type and concentration affected the phase behaviour of solutions. Their findings suggested that the addition of Cl based salts to their solutions of C8–Lecithin caused the temperature at which the cloudy phase was formed to first lower and then raise as the salt concentration was increased. Also, Taratuta et al. [28] noticed that the salt type and concentration affected lysozyme based protein–salt solutions by causing a linear increase in the cloud point with increases in the salt concentration. The salt type also had a big influence on this behaviour by increasing the gradient of this relationship when under constant total ionic strength and pH of the buffer [28]. Comparing the concentration of the salt to the cloud point temperature, NaCl has the smallest gradient, whereas solutions containing NaBr and KBr had much greater changes in cloud point with respect to increases in salt concentrations. This was a fact that also factored into the choice of NaCl as the salt because with a smaller gradient, the errors in the salt concentration will not have as large an impact on the cloud point determination. It was also found that this linear relationship only holds for monovalent cations and does not occur when divalent

cations such as Mg are used. In the case of a divalent cation, the cloud point temperature increases to a maximum before decreasing at high salt concentrations [29]. It was decided that staying away from these systems would be beneficial and that only monovalent systems were considered for use as the salt in this project. Also worth noting was that the concentration of NaCl added to the solution could be increased to much higher values than that of the other salt types tested (KBr and KCl). This was mostly due to the fact that potassium salts have a greater tendency to promote crystallization of lysozyme compared with sodium based salts. Again, this is good news for the choosing of NaCl, as the crystal formation is a process that is not wanted when imaging the phase boundary. The crystals will increase scattering within the sample and alter the localised lysozyme concentrations at positions of crystal formation [30] (also see Figure 18 where images from this project confirm this nature). As a result, potassium based salts were not used in this project and sodium was chosen as the monovalent cation to be used in this project.

The choice of salt was hence narrowed down to either a NaBr or NaCl salt. In order to narrow the decision further, the effects of using Cl and Br as the salt anion had to be investigated as this could also influence the behaviour of the sample. Cl and Br atoms have different degrees of hydration caused through the differing size of the ions (the smaller the ion the more hydrated it is) [31]. The larger the anion is the more effective it is at associating with the positively charged lysozyme surface. As a consequence, these anions are more efficient at screening the electrostatic repulsion between protein molecules. This causes an increase in the cloud point temperature (in line with the Hofmeister series) [31, 17, 32]. Therefore a Br anion in the salt would be expected to increase the cloud point temperature. However the differences between Cl and Br are not very large and as a result the choice between the use of Br and Cl in this project was trivial and in the end the choice of Cl was made. This choice was not based on the differences with Br but eventually on its availability in the lab seeing as the differences between Cl and Br were

fairly insignificant and do not effect the behaviour examined in this project greatly.

Further to this research, work by Muschol and Rosenberger [14] confirmed this choice of salt type. They performed experiments into lysozyme–NaCl solutions, testing the phase behaviour of the solution to changes in salt and protein concentrations. Using a similar experimental procedure to the one attempted in this project, they were able to create phase diagrams for 3%, 5% and 7% w/v NaCl concentrations. See Figure 1. At NaCl concentrations of 7% w/v, the phase boundary describing the onset of the cloudy phase was located at just over room temperature for concentrations between 60mg/ml and the critical concentration (found to be at approximately 260mg/ml). This is ideal for the conditions that are replicable in this project and as a result only concentrations of 7% w/v NaCl were explored in this project. This was also confirmed by Manno et al. who found agreement with Muschol's results when using an almost identical synthesis method [15].

2 Experimental Equipment and Techniques

2.1 Introduction

In order to image and acquire data on the behaviour of the phase changes in the binary liquid a confocal microscope was used. The experiment was then expected to expand into the use of ptychography to investigate the mixing of the phases on the boundary and to use it to acquire information regarding any changes in refractive index occurring that were not visible using the confocal microscope. To create the heat required for observing this change in phase, a Peltier heater was used alongside some adaptations including a metal block to dissipate heat and using thermal paste for a more efficient heat transfer.

Unfortunately, due to unforeseen circumstantial changes and after detailed evaluation on the use of ptychographic imaging, the ptychography setup was not used in the final experimentation and was replaced by the use of the confocal microscope as the main imaging method. Before it was realised that the use of ptychographic imaging would be unachievable, the initial experimentation was designed to investigate whether the experimental setup and the liquid chosen was suitable for ptychographic imaging through the use of the confocal microscope. This involved performing preliminary experiments using the confocal microscope to assess the suitability of the liquid system for testing using the ptychography method. These tests included finding the best operating conditions and refining the testing methods using the confocal microscope before applying them to the ptychography setup.

When performing this preliminary experimentation it was found that the confocal microscope was more suitable for this project than initially thought and that it would be ideal for the investigations probed in this report. There were also time restraints in that the ptychography system was very complex and prone to many problems. Thus a lengthier amount of time would need to be allocated to

the use of it which could not be offered. As a result this project never progressed onto the use of ptychography. Had these problems not have occurred the use of ptychography would have still been beneficial to this report because its ability to investigate the phase changes in more detail (its ability to resolve refractive index changes) could have provided some interesting results.

All experimental work was conducted at the Research Complex at Harwell (RCaH); Harwell Campus building number R92. The life sciences laboratory was used for all synthesis and sample preparation work and the microscopy room was utilised for all imaging purposes.

This section will serve as a detailed breakdown of the methods and theory behind each component of the experimental setup. It will also include outlines of the chemical synthesis methods that were deployed.

2.2 Confocal Imaging

As mentioned previously, one of the imaging methods used was confocal imaging. This imaging technique is mostly used for its unique ability to image single planes or "z–stacks". These are essentially images of constant depth or "slices" of the sample being imaged. This is of particular use in imaging phase changes in liquids as it enables the phase changes to be viewed in a constant depth slice where the confocal microscope offers better accuracy in the imaging. This accuracy can be attributed to its ability to image through contaminants and unwanted features within the liquid. If ptychography was used, the transmission of light through these objects would cause large distortions. But as confocal imaging uses the reflected light and not the transmitted light, the imperfections below the slice being looked at do not interfere with the image obtained. This is mostly due to its ability to reject light that does not originate from the slice by the use of a pinhole (see Figure 3). Such contaminants and impurities could include dust

or fine particles on the lens/microscope slides or even those that exist in the liquid itself such as protein globules and unwanted features such as crystal formation.

In simple terms, the microscope operates through creating an image of two different depths in the sample. The first area is focused on a point along the focal plane and the second is at a different depth that does not lie on the focal plane. The light reflected from the second area is mostly rejected by a pinhole whereas the first area passes through with minimal loss in intensity. The first area is then made more intense relative to the second area through the use of a confocal light source.

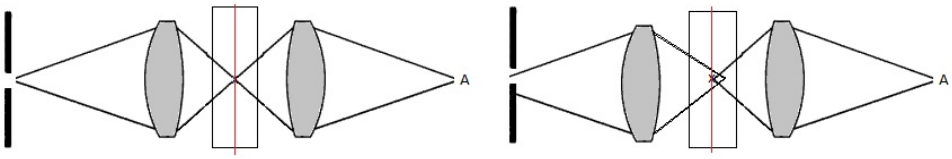

Figure 3: This diagram shows the basic principle behind confocal imaging. A represents the confocal light source origin. x represents the focal point. The red line represents the focal plane. The pin hole is represented by the dashed black line on the left of each setup and the lens by the grey shapes. The thin black lines going through the lens and focusing on x represent the path of the light source.

Figure 3 shows a simplified diagram of the process. The image on the left represents how the first image (the focused image) is formed. Light is focused onto the focal point which is then focussed within the pinhole

The image on the right represents how the second image is formed. The light in this case is not focused onto x but is focused onto a different depth (on a different focal plane). This unfocused image will be focused not entirely onto the pinhole and as a result the light intensity through the pinhole is reduced.

In both cases, the second (confocal) light source, originating from the point A, is focused on the original focal point (x). This intensifies the light that is received through the pinhole from the point x and also acts to reduce the intensity received by the unfocused beam. This results in a sharper image of the focal plane, providing an image that is only focused on a single depth.

By cycling through different depths (z planes) an idea as to the 3D structure can be obtained. This process of creating a series of single slice images is known as "z–stacking".

For more information regarding the theory behind this imaging technique, the reader is encouraged to read "Confocal Optical Microscopy" by R H Webb [33].

The equipment used in this project was an Olympus LEXT OLS4000 3D Laser Measuring Confocal Microscope. In LASER acquisition mode, a 406nm Semiconductor LASER was used which offered a maximum field of view of 16x16μm. This microscope also had a colour mode which operated by using a White LED to provide the light source, although this mode was used for qualitative purposes only due the inability to extract data from the images and its inability in imaging the changes in phase.

This microscope model was not designed to image liquids, its original purpose and specialisation was in the imaging of solid surfaces. This meant that its operation had to be adapted to suit this project. For the imaging of liquids the continuous mode was not useful as the software created images based on what it perceived was the surface of the structure. Without any solid structures in the liquid the imaging method often failed. Also the facility to create "z–stacks" was not included with the microscope software and had to be created through the use of the remote development kit (RDK). More information on this is included in the final results and in the appendix where the code for single slice imaging is

displayed. See Page 66.

2.3 Stage and Heating Method

Ideally, investigations into phase boundary behaviour require very accurate control over all of the variables that cause the unique phase changes. This is because the phase behaviour of a liquid will react strongly to very small changes in the variable conditions. In order to view fluctuations on a phase boundary these variables must remain as close to constant as possible throughout experimentation. These variables can include temperature, pressure and concentration. The lysozyme–NaCl solutions vary only with temperature and concentration of the sample and are not as strongly affected by pressure. By holding the concentration at a constant value and varying the temperature it is possible to probe the phase behaviour of the samples. This variable was controlled by using a Peltier heater (Farnell, cat no. 1639757 19V), a metal block (5cmx3cmx1cm), thermal paste (RS, cat no. 554–311) and a power supply (ISO–TECH IPS 2010). In order to understand the temperature response of the Peltier heater a digital thermometer was used (Thermco, cat no. ACC370DIG).

A Peltier heater consists of two semi–conductor materials (one a N–Type and the other a P–Type material) sandwiched between two metal heat plates. These materials are placed parallel to each other and are connected to a DC power supply so that the materials are connected in series. The cold plate absorbs heat from its surface and causes the electrons to move from the lower energy level (P–Type semi–conductor) to the higher energy level (N–Type semi–conductor). They are then pumped back to the P–Type semi–conductor through the use of the connecting power supply. This means that a temperature differential is created between both sides of the Peltier heater causing a hot and cold side to form.

By connecting the Peltier heater to the power supply and allowing it to ac-

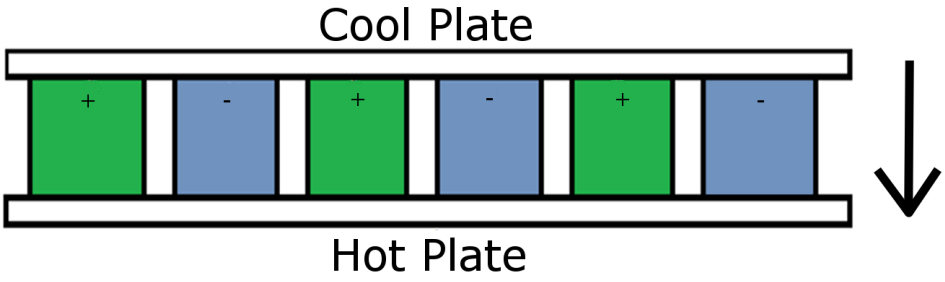

Figure 4: This figure describes the typical operation of Peltier heater. The electrons absorb heat energy at the cold plate causing a transfer in energy to the hot plate; the arrow represent the flow of electrons caused by this. The electrons are then pumped back by a connecting voltage in a direction opposite to the arrow. The "–" sign represents an N–Type semi–conductor material and "+" sign represents the P–Type semi–conductor.

climatise to the temperature of the surrounding environment, the temperature dependence of the heater can be kept constant. If the conditions change, e.g. the room temperature increases or the surface that it is mounted on (in this case a metal block) increases in temperature, the Peltier heater will respond differently to the supplied power. The effect of change in the surrounding environment can be eliminated through ensuring that the temperature of the laboratory was constant throughout testing. This would ensure that any data recorded was subject to the same conditions and would allow for fairer comparisons between data taken on different days. In this experiment the temperature was found to be the same value on all days of testing which eliminated this problem.

The operation of the heater requires a temperature differential between the hot and cold sides that is approximately constant, to achieve this a metal block was placed underneath the cold side. A metal block was used because its high thermal conductivity acted to shift the temperature of the cold side to reduce temperature fluctuations. A thin layer of thermal paste was applied between both the metal block and the cold side of the heater and in between the sample slide (where the samples were placed for investigation) and the warm side of the heater.

This helped facilitate more efficient and even energy transfer between the surfaces. This is an important part of the experimental setup as encouraging an even energy dissipation reduces the chance of localised temperature gradients within the sample. It also means that the images produced do not inaccurately portray the behaviour of the sample at what is assumed a constant temperature. If the sample had areas of different temperature, the phase changes shown by the imaging technique would not be representative of the temperature of the area predicted by the heating method.

When recording the temperature response of changing the voltage of the Peltier heater it is important to investigate the hysteresis of the heating system. This was done by cycling the voltage of the heater from 0V to 0.6V for five cycles. This enabled the evaluation of the stability of the heating system as it is cycled up and down in temperature and also allowed the investigation into the effects of the heating over long periods of use. These results are shown on Figure 6, Page 63.

The temperature and current were recorded for increments of 0.01V before being reduced back to 0V at the end of each cycle. A waiting time of 20 seconds in between each increase in voltage and a 10 minute waiting time at the end of each cycle was used to allow the temperature to equilibrate. 0.01V was chosen as the incremental size as this value was the smallest increment that the power supply could offer – although going to smaller increments would give more temperature control. To control the voltage increases a simple mouse macro was used alongside the computer software that controlled the power supply to ensure stricter control in the accuracy of the timing; resulting in fairer comparisons between cycles. These results showed that the starting temperature increases with each cycle and that the different cycles have different temperature responses (especially at low voltages). This was due to residual heat remaining in the metal block after heating to the highest voltage. This caused the lower voltage temperatures to have different values for each cycle as the metal block was at a different temperature than in

the cycles before. This could be improved by allowing a greater time between cycles, but this was not done in this project as testing the hysteresis behaviour with smaller times between cycles and for multiple cycles replicates similar conditions to what would be used in the final experimentation.

As the cycle number increased the temperature dependence converges into a stable response. This occurred around cycle 3 (as shown in Figure 7, Page 64) where cycle number 3,4 and 5 had a similar temperature response. It is assumed that the temperature dependence of the heater had stabilised in this region. As the behaviour converged after two cycles, in all future experimentation the heating system would be cycled equivalently before the imaging commenced. This would mean that the heating in all future experiments would start on the third cycle – a reflection on the relative stability of cycles 3, 4 and 5.

The results of cycles 3, 4 and 5 were averaged and then plotted onto Figure 8, Page 65. This formed the final temperature dependence graph which was used for calculating the temperatures in all of the experiments – provided the system went through two cycles prior to imaging to replicate similar conditions. This graph can only be used for voltage ranges between 0V and 0.6V, if the highest voltage differs from 0.6V, the temperature of the metal block when relaxed back to 0V at the end of each cycle will be different and the corresponding hysteresis behaviour will differ. Thus this temperature dependence is only valid for this particular system and a new experiment will have to be done for any different ranges.

The phase behaviour of the lysozyme–NaCl solution is not only dependent on temperature but also with concentration. Initially, the samples were treated to ensure constant concentration; this was achieved using two methods which both involved the enclosure of the sample from external effects such as evaporation and contamination. At first, the hanging drop method was suggested. This method would treat the constant concentration problem but as the liquid was in contact

with air, dissolution of $C0_2$ could increase the pH of the samples. Also there would be lensing and gravitational effects caused through the shape and thickness of the droplets. When initial testing was done on a droplet of the lysozyme–NaCl solution it was noticed that the convex surface of the drop caused distortions and the appearance of rings within the images (from the slices measuring constant height contours of the droplet edges). To fix this a cover slide would have to be used to flatten the surface which cannot be done using the hanging drop method. Also the thickness of the droplet would be too large, causing the high density phase sink with gravity (introducing 3D effects). This would then create an unwanted concentration gradient within the sample and spoil the response of the liquid. In this project the use of a 2D approximation is imperative in reducing these thickness dependant effects, as a result the method was rejected

To combat these failures in the use of the hanging drop method, a second method was devised. This involved the creation of a simple enclosure for the sample, consisting of a platform around the liquid and a cover slide placed on top. This meant that the sample would be trapped and isolated from external influences. Initial experimentation utilised this method, but it was later discounted as the sample depth was too thick and the higher density phase was sinking under gravity below the low density phase – this is the same as what was happens in the hanging drop method. This meant that imaging the sample variations with depth and temperature caused a time dependence as well. The depth of the enclosure could not be adjusted using available resources so the idea was not used for later testing. Instead a larger sample size was used with a cover slide placed on top. The focal point of the imaging was also set to the middle of the sample to reduce the effects of evaporation and contamination on the microscope edge. This also enabled the sample to be spread out thinner than before, allowing the approximation of a 2D system and thus reducing the complex depth dependent mixing that is present in thicker samples.

2.4 Synthesis of Lysozyme–NaCl Mixture

Part of the reasoning behind the choosing of the lysozyme–NaCl binary liquid system was for its relatively simple, quick and non–hazardous synthesis. This section will provide a detailed explanation of the experimental techniques that were deployed to produce the samples required for testing.

The materials used included: A NaAc buffer solution; pH 5.2±0.1 at 25 °C, 3M, 0.2μm filtered (Sigma Aldrich SKU = S7899, size = 100ml). Lysozyme powder; dialysed, lyophilised powder, 100000 U/mg from chicken hen egg whites (Sigma Aldrich SKU = 62970, size = 1g). And NaCl powder; purity ≥99.5% (Sigma Aldrich SKU = S7653, size = 250g).

Before the imaging of the liquid, initial experimentation in the lab was spent focusing on understanding and developing a simple method to create it. The first methods attempted were based on the methods used by Muschol and Rosenberger [14] and Manno et al. [15]. First, 1ml solutions of the 0.1M NaAc buffer solution were prepared by diluting the NaAc buffer solution from 3M to 0.1M using distilled water. NaCl powder was then dissolved into these solutions by using a vortex (MyLab SLV–6 Vortex Mixer) to encourage dissolving. These solutions were then heated to 45 °C using a block heater (Stuart Block Heater SBH130D).

To ensure that the temperature of the NaCl–NaAc solution was 45 °C a separate eppendorf containing distilled water was placed in the heater and a thermometer was used to measure the temperature of the water. When the temperature reached 45 °C, the Lysozyme was mixed into the NaCl–NaAc solution by hand to encourage dissolving. In order to weigh the amount of lysozyme accurately, the required amount was dispensed into a small measuring container which was weighed on a scale (Denver Instrument S1–234). Then, the contents were dispensed into the eppendorf containing the NaAc–NaCl solution that was just made. The mass of the now mostly empty measuring container was then re–weighed and subtracted

from the original mass to obtain the true amount of lysozyme that was successfully dispensed into the eppendorf. This method was also used for any additional adjustments to this quantity until the required amount was reached. This technique for weighing the lysozyme was used throughout all of the experiments including the weighing of NaCl that was added to the solutions. This method accounts for residual mass that is retained in the measuring container which allows for greater accuracy in the quantities added.

This solution of lysozyme, NaCl and NaAc was then vortexed until the clusters of Lysozyme powder were not visible and was then placed inside a centrifuge (eppendorf Mini Spin Plus) at 7500rpm for 10 minutes to help remove undissolved protein, air bubbles, and dust.

This method was then improved by creating a large (10ml) stock solution of this 0.1M NaAc buffer solution to reduce experimental errors in the molarity of the buffer solution. This was done by diluting 330μl of the 3M NaAc buffer solution with 9660μl of distilled water. This solution was then vortexed for 30 seconds on a high speed setting to mix the solution together.

In this project only NaCl concentrations of 7% w/v were tested, this meant that the NaAc buffer solution would always have 7% w/v NaCl dissolved in it. With this in mind, the next step in the developing of the synthesis method was to dissolve this quantity into the 0.1M NaAc buffer solution to obtain a large stock solution for use in further experimentation. To do this a new 10ml solution of the 0.1M NaAc solution was created using the same method as above and 7% w/v (0.7g) of NaCl was added to the solution which was then vortexed on a high speed for one minute. This allowed for greater accuracy in the quantity of NaCl dissolved in the solution as the experimental errors are a smaller percentage of the total quantity when the sample size is increased. Alongside this improvement future samples were no longer centrifuged, this is because the two concentrations

of lysozyme present in the cloudy phase were separated by the centrifuging process. Samples taken from the bottom of the eppendorf were highly concentrated compared to the top of the liquid, this meant that the concentration of the samples taken from this solution were unknown. Without knowing the concentration of lysozyme in the samples taken from these solutions it is impossible to conduct the required experimentation in this project.

By using high concentrations of Lysozyme (>150mg/ml) the solutions became very dense and gel–like. This is most likely the same gel formation as described by Muschol et al. [14]. This gel–like structure inhibits the liquid from going through the phase separation. This is not a regime that is wanted and as such only concentrations below this value were used after this realisation.

After much research into the literature surrounding the synthesis of lysozyme–NaCl solutions, the mixing technique was also changed. The use of a vortex created violent mixing which increased the chances of the protein denaturing, thus altering the behaviour of the phase separation and crystal growth chances [34]. As a result, the vortex was no longer used for mixing the solutions. The lysozyme was mixed into the solution by heating and maintaining the solution at 45 °C and gently mixing by hand every 2–3 minutes until visibly dissolved. Ideally a low rpm Thermo–shaker would be used however over the period of this experiment, the equipment was always either broken or in use. If one was to be used it is recommended that settings include an incubation temperature of 45 °C and a rpm of 100.

3 Results

3.1 Initial Experimentation

3.1.1 Introduction

Before the main experimentation commenced, the first series of experiments (spanning to roughly before Christmas) were spent designing the experiment to be performed, ordering equipment and chemicals and creating risk assessment forms. As well as this, a significant amount of time was spent performing initial experiments on the confocal imaging equipment to gain a better working understanding of its operation and limitations and to ensure that the experimental setup and environment were suitable for its operation. Initial experiments were also designed to test the effectiveness of the synthesis method improvements as discussed in Section 2.4 and to perform simple imaging tasks of the lysozyme–NaCl mixture.

For a long period of time at the beginning of the project, the experimental setup was limited in that one of the software keys for the confocal microscope had lengthy delays in delivery from the manufacturer. This meant that some of the features of the software including the ability to capture slices of the samples were unavailable. Hence most of this initial testing was designed to make use of the already existing functions of the software (including the continuous scanning mode). As a result most of this testing was done on the crystal growth and dynamics observed in the lysozyme–NaCl mixtures and not on the liquid–liquid phase boundaries (as the continuous method could not image the liquid successfully).

This section will describe the limitations that were uncovered and will also describe some of the first data that was acquired regarding the initial lysozyme–NaCl samples.

3.1.2 Crystal Imaging Using Continuous Scanning Method

At the beginning of the project time–line initial experimentation was spent without the use of the constant slice mode of the confocal imaging equipment and all work had to be completed using the continuous scanning mode. The continuous scanning mode was a feature of the equipment that enabled the imaging of a sample based on the software's interpretation of finding the top surface. This is used primarily as a surface roughness calculator and is a very powerful tool in resolving information on the surfaces of solids. The method worked by scanning over a specific depth range and taking slices with a certain frequency as defined by the user. Based on the intensities of the scanned range, the software locates and creates an image of what it believes to be the top surface. Although a powerful tool when imaging solids this mode of scanning is not as useful in experiments performed on liquids as there are no solid surfaces in the liquid. Thus when imaging a liquid, the software identifies false "top surfaces" which are in actual fact a random slice within the sample. As well as this limited control over the imaged area, the resultant slice has no depth value associated with it and as a result, the location of this top surface image is unknown. When imaging the liquid, the images created were often focused onto the cover slide as the software determined this as the top surface, meaning that the images produced often did not contain any data regarding the liquid below the slide. These images were characterised by either producing over saturated images – due to the large intensities of reflections from the cover slide, or blank images – where the software automatically reduces the brightness of the images to zero to protect the sensitive detector. See Figure 9, Page 81 and Figure 10, Page 82 for examples. This method clearly wasn't working. In order to image the liquid the z–stacking method would have to be used.

After this failed experiment and until the software key arrived, time was instead spent imaging the crystal formation in the lysozyme–NaCl mixtures.

It was noticed that the solutions were able to create crystals of an tetragonal

structure when the solutions were incubated at approximately 3 °C. These solutions were made using the original synthesis method as described in section 2.4 (paragraph three and four) using 178mg/ml lysozyme in a 7% w/v NaCl solution of 1ml, 0.1M, pH 5.2 NaAc (the NaAc and NaCl mixtures were not from a pre made stock solution but were created separately for each sample).

Samples were left in a fridge for two days to allow the crystals to form and were imaged by placing a sample of 30μl on a glass microscope slide and covering with a thin cover slide. The samples had separated in the fridge as the conditions that they were kept in were well within the cloudy phase. This separation was due to the high density phase sinking below the low density phase under gravity. As a result, the crystals in the bottom of the samples were larger as there was more lysozyme available for crystal growth whereas crystals on the top were found to be smaller. Figure 11, Page 83 and Figure 12, Page 84 display this difference visually. Figure 11 shows the crystals generated from the bottom of the separated solution and Figure 12 displays the upper crystals that were formed. These images were created by taking screen–shots of the live display as the continuous scanning mode only focussed on the cover slide.

Figure 15, Page 87 was created when this solution was mixed by vortexing under a very low speeds. In this figure it is easy to see the variation of crystal sizes that were formed. However it should be noted that the vortexing procedure may have influenced this range of crystal sizes. This is because the crystals would have collided with eachother and the walls of the container when being vortexed causing them to break up on impact into the various sizes shown.

By locating clear crystals within the samples and utilising the LASER continuous scanning mode of the confocal microscope, various images of the crystal structure were made. Examples include Figure 13, Page 85 and Figure 14, Page 86. From these images it is clear to see the tetragonal structure. This result is ex-

pected when comparing to Muschol et al. [14] who proposed that tetragonal structures were formed below 25 °C. Orthorhombic crystal structures can be formed by altering the incubation conditions (see Figure 1, Page 14), however when using very high concentrations of lysozyme, the temperature at which this occurs is very high and impractical unless the concentration of lysozyme is reduced considerably.

Another interesting result was that the temperature at which the crystals started dissolving occurred at around 89V (41 °C) with complete dissolving achieved at 1.22V (55 °C). This was calculated by increasing the power supplied to the Peltier heaters until the crystals started to lose shape and melt slowly into the solution. Comparing this to Vasylkiv et al. [35] gives a disagreement to their expected dissolution temperatures of 34 °C (the start of crystal dissolving) and 50 °C (completely dissolved). This difference could be due to a number of reasons, however the most likely reason is that the temperature measuring system is not reliable. This is because at higher temperatures, the metal block will not be able to dissipate enough heat to counteract such large increases in the power delivered to the Peltier heater causing the error in temperature calculation to increase. Another equally plausible problem is in the measuring of where the dissolving begins and ends. In this experiment it was found to be where the image started to haze around the crystal as it was being dissolved. Also very small changes in size were noticed. The upper temperature associated with this dissolving is also very hard to define as the higher temperatures merely state an increase in the rate of dissolving. Therefore the time that the sample is under heating comes into account. This is a problem with the measuring and should have been noticed and addressed at the time of experimenting. The issues with this method were not realised until very late in the project and rectifying this could not be completed. The methods outlined by Vasylkiv et al. [35] should have been followed and because they were not, the values obtained in this experiment are stated but not presented as definitive.

3.2 Imaging The Cloudy Phase Boundary

3.2.1 Introduction

In order to image the phase boundary behaviour of the lysozyme–NaCl solutions experiments were performed to investigate how the light transmitted through the sample changes with temperature (and hence phase), additionally experiments were performed to locate the phase boundary of the cloudy phase. Then attempts were made to image the phase boundary of the cloudy phase by holding the temperature of the sample on the phase boundary (as determined by previous experiments).

3.2.2 Effect Of Temperature On The Intensities Of The Slices

As mentioned previously, the ability to measure the liquid using the confocal imaging equipment hinged primarily on its ability to get single slice image data. Initially this was not possible and it was only at around mid–January that the RDK software key was available. This was because the ability to perform single slice imaging required the use of the RDK to control the operation of the microscope. The use of the continuous mode was not suitable for imaging liquids and produced images that weren't usable like Figure 17, Page 89 – this image shows what appears to be the top of a glass cover slide. This mode was useful for imaging crystal structure (as in Section 3.1.2) but not for the imaging of liquids. Before this key arrived an with time slowly ticking away a temporary fix had to be created so that the project could progress.

To overcome the problems with the imaging mode and successfully image the intensity and phase behaviour of the liquid, a piece of screen–capture software called "CamStudio" was used to record the live output of the scanned area. This proved to be a successful solution and images were obtained as required however there were many problems with this technique: The images were not very accu-

rate as the frame rate was low and the images were heavily compressed by the software. This meant that the intensities of the images were not representative of the raw data as acquired by the confocal microscope. Luckily the RDK software key arrived within two weeks of attempting this solution, meaning that single slice imaging could now be attempted.

The RDK works by sending commands from an external computer to the host computer. The host computer is the computer that is connected directly to the confocal microscope and is the computer that operates the software that controls the microscope. By sending commands over the network using the RDK, one can bypass the limitations of the software and create scripts to perform automated tasks including the ability to perform z–stacking.

Through learning the operation of the RDK and the codes that would be required it was possible to create a working code that when sent to the host computer would initiate the z–stacking/slicing of the sample. For the purposes of this project the code was required to include the exporting of uncompressed .tif images and the raw intensity data (.csv files) of each image. It wasn't possible to export the raw data directly using the RDK as the raw data would only get exported as a profile measurement and it was not possible to export the intensity data relating to the images. Instead, the data had to be saved manually after the scans had finished. To speed up this process a mouse macro was created that automated the saving process. The resultant .csv files contained the intensity map of the images produced, with intensity values given for each pixel that was measured. The resolution was 1024x1024 which resulted in over one million data points per image. This was an extensive volume of data to process so a script was created in VBA to sort the data into one big Microsoft Excel workbook to save time (see Section 6.2.2 for the code). This code compiled all of the .csv files into one workbook with each image's intensity map on a separate spreadsheet. The total and average intensity of each slice was computed and compiled onto a new sheet with all of the

other slices' results. This allowed for easy importing into MatLab for graphing and other data analysis purposes. A sample script describing the z–stacking code is given in the appendix; see Section 6.2.1.

The initial tests into the imaging using the slicing software were unsuccessful, experiencing both problems with the RDK as well as the tested lysozyme–NaCl solutions. The RDK was able to perform the commands called by the script, however it often doubled up the distance between slices and often chose the magnification lens randomly. Extensive effort was spent trying to rectify these problems and many methods were attempted but none seemed to prevent them from occurring. Often scripts that were fully working a day before would not work and would exhibit this random behaviour. A fix was not created and the effects were uncontrollable, the only way to fix it for a session was to clear the log and restart the computer a few times. This stopped them from occurring throughout an imaging session but the original cause of them is unknown and still persists.

The majority of problems, however, weren't down to the slicing scripts but the synthesis of the lysozyme–NaCl solutions. As a result the synthesis method was evolved to prevent them. Initially, samples were re–used over the period of a couple of days so that the imaged behaviour could be reproduced and confirmed. This involved heating the samples past the crystal dissolving temperature to dissolve the unwanted crystals. But by doing this extreme heating the samples no longer exhibited phase separation. It was not known at the time that this heating was the cause of the problems until extensive research suggested that this heating caused gelation of the solutions which was inhibiting the phase behaviour. This was documented by Muschol et al. who noticed that this heating caused a gel phase which prevented the normal phase separation occurring [14]. To avoid this, samples were instead created fresh at the start before each imaging experiment.

Also, crystal formation was found to increase when the sample was kept un-

der the cloud point temperature (also found by Muschol et al. [14]) and that it increased further when held on the phase boundary. This often led to crystal formation in lengthy experiments; an effect that causes localised lysozyme concentrations to vary in time (the crystal formation absorbs lysozyme which reduces the localised concentrations). As a result the data collection period was shortened to reduce the influence of crystal formation on the concentration of lysozyme in the solution. It was also noted that this increased crystal growth rate at the phase boundary would probably lead to problems when imaging the liquid on the phase boundary (the main premise of this project).

These newer samples were created by by making a large stock solution of 7% w/v NaCl & 0.1M pH 5.2 NaAc and then dissolving the lysozyme using the last method described in Section 2.4 (no vortexing or centrifuging).

With these adjustments, the samples exhibited more stable behaviour and worked until two weeks later when the samples showed no phase changes. Tests were then conducted to find the problem. The lysozyme powder was changed to see if the previous sample had been denatured or had been contaminated; it was stored in an area used to store many other chemicals so the chance of contamination was high. Also the microscope and cover slides were changed in case contaminants and impurities were present that could have interfered with the lysozyme–NaCl solutions or the imaging process. As well as these, the NaCl–NaAc solution was recreated to test if it had been either: contaminated, if the solution had evaporated through repeated opening or if the solution had been stored incorrectly. New samples were made that tested each of these potential problems by changing them one by one until the issues ceased. In the end it was found that the NaCl–NaAc solution was the problem and the creation of a new stock solution solved the phase change issues.

Changes were also briefly made to the application method. Before now just

a cover slide was used to isolate the samples, to improve this method a better technique was devised. This involved creating a platform around the sample and sealing it with a cover slide. This method decreased effects such as the evaporation of the liquid and the dissolving of CO_2 into the liquid. However the added depth of the sample introduced gravitational effects and caused the mixing of phases to vary with depth. This was a very complicated regime that was not wanted for the purposes of this project. As a result, this method was scrapped in favour of using just the cover slide. This application method is described in more detail in Section 2.3.

Also the solutions (dispensed at 45 °C) were initially placed onto a cold microscope slide. This caused them to change temperature upon touching the slide and caused it to enter the cloudy phase (which is more viscous than the clear phase). This meant that when the cover slide was placed on top of the sample, pressure on the top was required to create a thinly spread sample. This pressure could not be applied uniformly and often caused unwanted lensing effects in the imaging due to the uneven separation between the cover and microscope slide (Newtons rings effect, see Figure 18). To solve this problem the microscope slide was also heated to 45 °C to prevent this temperature change and to promote a thinner sample spread.

Having solved numerous problems with the solutions, the slicing software and the application method the experimental testing could begin. Using these revisions to the synthesis method and sample application, a 1ml sample of 100mg/ml of lysozyme in a 7% w/v NaCl, 0.1M pH 5.2 NaAc solution was made (of which 20μl was applied to the microscope slide for testing). Whilst this solution was made the Peltier heater was cycled through the first two cycles of heating to prepare the heating system for testing. This was done in order to recreate the conditions for stable temperature measurement (see Section 2.3). Before the z–stacking script ran, the top of the sample (defined as just under the cover slide) was located and the depth was noted down. The depth at which the liquid started was input into

the z–stacking code as the starting point for imaging. 18 slices through the sample were formed using the z–stacking script which ran for Peltier voltages ranging from 0.36V ($28.1 \pm 0.3\,^{\circ}$C) to 0.50V ($30.8 \pm 0.3\,^{\circ}$C) in steps of 0.01V. The data was extracted, compiled using the VBA script and then analysed through the creation of various graphs using the MatLab code as described in Section 6.2.3. A graph comparing the Intensity variations with depth of the 100mg/ml lysozyme solution is shown on Figures 19, 20 and 21 on Pages 91, 91 and 92.

The confocal microscope images the higher density phase of the mixture as being darker than the low density phase due to the differences in refractive index of the phases. Therefore when the liquid exists in the cloudy phase (the point at which the solution separates into these high and low density phases), the total intensity of the resultant images are expected to be lower than in the clear phase where there is no refractive index difference. The data obtained from the experiments into this behaviour agree with this well; as can be seen in Figure 19. The total intensities of the clear phase are on average higher than those for the cloudy phase. There is a period between slices 9 and 13 where the average intensities are instead higher for the cloudy phase although this can be attributed to the auto exposure feature of the software which was used in the slicing scripts. Slices where the average intensity was over a threshold value at the beginning of the imaging bypassed the auto brightness feature and remained at their brightness level. It is only when the system senses an average brightness lower than the threshold or if the intensities over saturate the detector that the auto exposure function changes the brightness of the images. In the case of the clear phase, the intensities were high enough at slice 9 that saturation occurred (the intensity reached over 9×10^8) and the brightness was automatically reduced by the software. This was not seen in the cloudy phase as the intensities were generally lower and not significant enough to cause over saturation and trigger the automatic brightness adjustments; see Figure 20 and Figure 21. When comparing these graphs it is clear that the intensity of the cloudy phase drops off quicker than the clear phase,

occurring at around slice 12 for the cloudy and slice 15 for the clear phase. In this experiment the distance between slices was set at 2μm meaning that the clear phase can enable the resolution of an extra 6–8μm of depth compared to the cloudy phase.

Data was also obtained for lysozyme–NaCl solutions containing 60mg/ml and 80mg/ml of lysozyme in solution. These solutions were created on different days using the same synthesis and application methods as well as the same experimental setup used in the 100mg/ml lysozyme solution. The usual procedures were followed prior to starting the experiment including cycling the Peltier heater through two heating cycles and performing an initial experiment to find the top of the liquid sample. Due to time restraints but also to reduce the influence of crystal formation, the data collected for the 60mg/ml and 80mg/ml concentrations only investigated two temperatures – one low and one high temperature describing behaviour well within the two phases. Also a larger range of slices were taken to ensure that the features of the liquid in these cases could be matched against the features in the 100mg/ml case. This allowed the point at which the intensity dropped off to be shifted and aligned with the 100mg/ml data for easier comparison. As a result the slice number for each case does not correspond to the same depths into the samples and should be remembered when comparing the data. The distances between the slices does however remain the same at 2μm. The high and low temperatures probed were 0.23V, $25.4 \pm 0.3\,^{\circ}$C (80mg/ml) and 0.13V, $23.4 \pm 0.3\,^{\circ}$C (60mg/ml) for the cloudy phase, 0.37V, $28.2 \pm 0.3\,^{\circ}$C (80mg/ml) and 0.27V, $26.2 \pm 0.3\,^{\circ}$C (60mg/ml) for the clear phase. The temperatures were calculated using Figure 8 on Page 63. The results are plotted on Figure 22 on Page 92. The data obtained for the 60mg/ml and 80mg/ml cases show very similar behaviour to each other and the 100mg/ml case and with the intensity drops matched to each other it is clear to see the similarities between the intensity behaviour between the samples. All three solutions exhibit very similar intensities in the lead up to the intensity drop. There are also remarkable similarities in the

60mg/ml and 100mg/ml cases whose intensity variations follow the same pattern of peaks and troughs in the high temperature environment. This behaviour is very interesting yet remains unsolved as further testing on this behaviour is required in order to see if the behaviour is replicable.

As only one successful experiment was made for each protein concentration, the data that is displayed cannot be described as absolute and definitive of the true behaviour of the samples. Multiple repeats of the experiments are required in order to gain averaged information and to assess whether the data is accurate and not anomalous. As well as this, it is worth noting the errors and problems that can be associated with the data. The experimental errors include variations in concentration and pH associated with both the contact of the solution with its environment and evaporation effects. Also, the concentration of NaCl used in the solutions is not absolute and contains a large experimental error associated with the creation of the solutions. There are also problems with the experimental setup including effects such as Newtons rings which cause constructive and destructive interference that can alter the intensities of the images. This effect is brought about through the change in viscosity that accompanies the change in temperature (phase). As the temperature of the solution is changed, the viscosity of the solution changes in response. This causes the cover slide to sink further into the sample and causes the angle between the cover and microscope slide to differ and no longer be parallel. This results in large sweeping dark sections associated with the destructive interference caused by the sloping cover slide. When these dark patches of intensity appear over the imaged area, they reduce the intensity of the images, masking the true behaviour of the liquid. See Figure 18 for an example of this behaviour.

The overall behaviour observed in this experiment was that the lysozyme concentration did not affect the difference in the intensity drop off between the cloudy and clear phases. This difference was approximately 6–8μm. There is also a noted

increase in intensity of the clear phase compared to the cloudy phase at the point just before the intensity dropped off. However this could be due to differences in the lensing effects in the clear phase where the cover slide sinks lower due to the lower viscosity phase. These lensing effects include reflections from the cover slide as it moves closer to the imaged slice (focal plane) when sinking. It is also noted that these results were only based on one set of results for each concentration of protein and is subject to further testing to confirm this nature.

3.2.3 Adjusting Temperature to Locate The Phase Boundary

Through the results of previous experimentation and by reviewing the literature surrounding the lysozyme–NaCl solutions, it was noticed that the crystal nucleation and growth rates affect the nature of the phase change behaviour. By testing solutions over large time–scales (typically those in excess of three hours) the onset of crystal formation begins to interfere with the phase behaviour as crystals absorb and lower the localised lysozyme concentrations (as witnessed in Figure 18). In order to reduce inaccuracies related to this behaviour it is imperative to ensure that the experimentation occurs over the smallest time frame possible. In this experiment the nature of the phase change needs to be as accurate as possible and not be affected by the crystal formation. This means that the ability to measure over a smaller time–scale is very important in this experiment and led to the use of imaging only a single depth for each temperature value. To find the optimum slice for the imaging, preliminary tests were performed on the samples before the final experimentation commenced. A slice had to be found that was safely in the middle of the visible liquid region where the intensity was large enough for the changes in intensities through changing phase to be noticed. Finding this slice was not as simple as guesswork as the problem of the viscosity change in the liquid at the different temperatures caused the thickness of the sample to vary. This was due to the pressure of the cover slide on the liquid no longer being in equilibrium with the buoyancy provided by the liquid at higher temperatures (clear phase

which is less viscous). This acts to displace more liquid and spread out the liquid more underneath it. When the cover slide depresses more into the liquid, an image depth in the cloudy phase may relate to an image in the clear phase that is very close to the cover slide. This causes more optical effects that distort and promote inaccuracies in the images produced. Also the glass slide may depress into the region of the slices themselves and one may image the cover slide by accident. In order to prevent this, slices must be taken from the middle of the liquid sample well away from the cover slide in both temperature regimes.

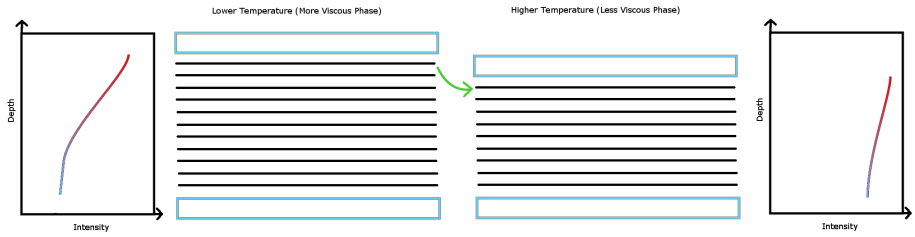

Figure 5: This figure describes why the image slices must be chosen carefully. The slices must be chosen to avoid taking slices near to the cover slide. This is because the cover slide depresses when the temperature is increased and imaging close to this boundary can influence the intensity of images taken. Optical effects like reflections from its surface and even mistakenly imaging the cover slide itself can lead to results that aren't representative of the true behaviour of the liquid. In this example, if one of the top 3 slices was chosen, the higher temperature image of the same depth would actually image the cover slide.

To find this "ideal" slice, the microscope was focused onto the cover slide and cycled past the cloud point into the clear phase. In this cycling, adjustments were made to the imaged depth to ensure that the microscope was always focused just on the underneath of the cover slide. Once into the clear phase, the depth was lowered to a point away from the influences of the cover slide and then cycled back down in temperature to ensure that the chosen depth was still in the middle of

the liquid and that the cloudy phase was still visible.

Initially, this took many attempts and different samples to get right as the images produced seemed to differ with each new solution despite using the same successful method as in Section 3.2.2. There was clearly something wrong with the synthesis procedure or in the chemicals themselves and another session was spent trying to understand the root cause of the problems. After testing the NaCl–NaAc solution, microscope slides and the lysozyme powder it was deduced that the problem was associated with the lysozyme powder and that the new lysozyme sample solved these problems.

With the solutions behaving as expected and a suitable slice found for the imaging, an experiment was set up to locate the cloudy phase boundary in the 100mg/ml, 80mg/ml and 60mg/ml lysozyme–NaCl solutions. This range was chosen as higher concentrations led to supersaturation and unstable phase effects. In fact before the concentrations were decided, most of the early samples created were highly concentrated (often >200mg/ml). These samples were close to/above the critical lysozyme concentration and showed no phase changes at the expected temperatures. The solutions also formed very viscous gels which were hard to dispense. Thus, the samples were created to avoid this regime by using a much lower concentration. By using concentrations lower than 60mg/ml, the phase boundary was found to be too close to the room temperature and as a result accurate temperature control was limited. At very low concentrations, the temperature would be below room temperature meaning that the samples would have to be cooled using the cold side of the Peltier heater. If the cold side was used then experimentation would be unfair as the heating method would have differed from the higher concentration samples. Thus a working range of 100mg/ml–60mg/ml was used.

With the standard procedures satisfied for ensuring accurate operation of the Peltier heater (two cycles of heating), the samples were placed into position and

imaged over a range of temperatures. The RDK script was adapted to maintain a constant depth and take a series of three images over a period of 9 minutes for each temperature setting. The temperature was then increased and the sample was allowed to acclimatise for two minutes before imaging was started again. In doing this, a series of three images per temperature were created and used to find the location of the phase boundary. This was then repeated for the other lysozyme concentrations. The divisional change in temperature was set to the smallest possible amount (0.01V changes applied to the Peltier heater) which although not small enough to thoroughly investigate the behaviour of the liquid, it provided a good indication of the location of the phase boundary. Examples of the images that were created using this method are included in the appendix, see Figure 23. This figure shows a series of some images created from the 100mg/ml lysozyme solution.

Through analysing the resultant images, a measurement of the phase boundary could be made. The exact point of the phase boundary could not be located as the temperature changes were not small enough. As a result, the phase change was located as being between the two images that described the behaviour of the liquid just below and just above the phase boundary. The phase boundary temperature was given as being half way between the two images' temperatures. This was calculated by plotting onto Figure 24 and reading off the temperature range between the two images. These temperature values also included the upper and lower bounds of the errors associated with the Peltier heaters.

This gave values of $28.65 \pm 0.35\,^{\circ}\mathrm{C}$ (100mg/ml), $26.35 \pm 0.45\,^{\circ}\mathrm{C}$ (80mg/ml) and $24.55 \pm 0.35\,^{\circ}\mathrm{C}$ (60mg/ml). These results were plotted onto a graph to compare with data from Muschol et al. [14] and Manno et al. [15], see Figure 25. Manno and Muschol used virtually the same synthesis as each other and a very similar one to this experiment. They used comparable lysozyme samples, a NaAc buffer solution of 0.1M and pH 4.5 and 7% w/v NaCl. The only difference between this project's synthesis method and their method was in the pH of the buffer solution,

which is noted as a potential reason for differences in results. Further to this graph, the data in this project and the data relating to Manno's and Muschol's experiments were fitted to Equation 1 using MatLab and the code in Section 6.2.4. This fitted curve is shown on Figure 26, Page 96.

When comparing these sets of data it is reasonable to state that the results obtained in this experiment agree with the experimental data collected by Muschol and Manno. The fitted curve falls within the experimental error and obeys a very similar trajectory to the fit for Manno et al. It differs mostly by a uniform shift down in temperature. This difference was initially thought to be due to the difference in pH of the solution, however after extensive research it was found that increasing the pH acts to linearly increase this boundary temperature (Taratuta et al. [28]), the opposite of what was initially suggested. It is worth noticing that the pH range tested by Taratuta to get this relationship only considered pH 5.6–7.9 and not the pH ranges compared in this report. As a result, the behaviour of the pH change for lower pH values may not fit to the same linear relationship as for the higher pH values assessed by Taratuta. This means that it is inconclusive whether the pH difference between this project's and Manno/Muschol's results were the cause of this shift. Further experimentation would have to be done to investigate the pH dependence on the phase boundary for a pH of 5.2 and 4.5 for a conclusive statement to be made. This systematic shift could also be due to the errors associated with the heating system. If the temperature of the metal block was cooler than when the temperature dependence graph for the Peltier heater was created (Figure 8) then a systematic shift to reduce all temperatures is expected. As the temperature of the metal block was not tested at the time of experimentation or when measuring the temperature response of the Peltier heater, then this effect cannot be ruled out. A difference in temperature could have occurred which would have been responsible for the shift. As well as these potential sources of error, it was also realised that the methods used in the synthesis of the samples contained lots of potential errors. Also, truly accurate temperature and

concentration control was not replicable in this project and could have contributed to this error. Improving this would require more time and resources than were available although some simple adaptations were noted for future reference and are discussed in Section 4.

Overall the results gained in this project agree well with the behaviour expected and produced a curve very similar to data from Manno et al. However, this data also showed a systematic shift of a lowering in temperature which could be down to the differing pH and the errors in measuring the temperature accurately. Repeat experiments (which were not performed due to time constraints), would assess the reliability of the testing method and would also allow the testing of the potential sources of errors to find the causes. Also, experimenting the effects of how the different pH used in this project affect the phase boundary would help in determining whether this shift is down to the pH.

3.2.4 Imaging Fluctuations On The Phase Boundary

After the successful experimentation into finding the phase boundaries, a series of experiments were setup to image the liquid on the phase boundary of the cloudy and clear phase. However, despite many attempts the conditions required for holding the liquid on this phase boundary weren't accessible using the equipment available in this project. Inadequate temperature control and insufficient isolation controls meant that due to the very sensitive nature of phase changes, holding the conditions perfectly was unsuccessful.

The samples used when this imaging was attempted were prepared in the usual way using the same synthesis and application methods a in the previous experiment. The Peltier heater was prepared through the use of the cycling procedure and the sample was placed onto the microscope stage ready for testing. 100mg/ml lysozyme samples were tested, however none were able to be held on the phase

boundary.

Multiple samples were created to assess whether the problems were due to the synthesis method; changes to the samples included using different lysozyme, NaCl and NaAc samples and different cover slides, however the problems still persisted. As a result, the problems were attributed to issues with the sample environment controls (controlling evaporation and contamination) and the heating accuracy of the Peltier heaters.

A series of images produced from one of the attempts is shown on Figure 16, Page 88. As shown, the samples either existed in the cloudy phase or the clear phase. The inability to resolve smaller changes in temperature meant that the temperatures within this range could not be exploited and the accurate conditions for the phase boundary could not be replicated. As well as this inability to resolve smaller changes in temperature, there were also influencing factors originating from evaporation of the sample at the edges (increasing the concentration of the samples) and in the contamination of the sample at these edges – including the dissolving of CO_2 (decreasing the pH of the solution). Problems of this type introduce time dependency in the phase boundary temperature and make it harder to hold the system on the phase boundary. Subsequently, for this type of experiment much better temperature control and isolation is required before success in the imaging can be achieved.

Although too late in the project time–line to implement a new heating system, it was possible to attempt a simple fix to prevent some of the other potential issues. The sample was placed inside a capillary (Hirschmann Laborgerate Haematokrit–Kapillaren, cat no. 9100160) and was sealed off at both ends with foil to prevent the evaporation and contamination issues. But the imaging was not successful using this method as there was an uneven surface in contact with the heater that introduced uneven heating within the sample. Also the curvature caused many

lensing problems which lead to unusable images and the thickness of the capillaries (0.95mm) introduced unwanted effects caused by the breaking of the 2D assumption (including gravitational effects and the mixing of the phases with depth). As a result this method did not succeed. Resultant images from this method are shown on Figure 27, Page 97 to show these problems.

4 Suggested Improvements To Methodology

There are multiple ways to improve the experimental setup used in this project and with more time and resources it would be interesting to compare these results with using improved methodology.

On the question of solving the temperature control issue a system of an "oven inside an oven" would greatly improve the accuracy of the temperatures achieved. This method would involve a properly insulated outer oven to control the temperature within it. A second oven within this oven would then be able to provide more accurate temperature control. This is because for the inner oven the difference in temperature between what it is trying to replicate and the environment that it is surrounded in is much smaller than when not immersed in the first oven. This results in an increase in temperature control as there are less fluctuations in temperature and small changes in temperature are more stable.

In order to address the isolation issues of the sample, the sample could be placed inside a sealed and sterilised environment. This would prevent contamination and evaporation from occurring and would help to keep the concentration and pH of the sample constant. Achieving this could involve the use of a capillary but when this method was tested in this project it was found that its depth and curvature caused problems with imaging (see Figure 27). This could be combated by using a sufficiently thin rectangular capillary where it has flat surfaces instead of a cylindrical shape (similar in shape to a hollow elongated rectangular prism). This would eliminate the lensing effects associated with the curvature of the capillary and if thin enough, would reduce the influence of the third dimension allowing the two dimensional approximation to still be valid.

Further experimentation could include investigating any polarisation and birefringence effects that are present in the samples. This can be achieved through the imaging of the samples across a range of angles to discover changes in the phase

behaviour of the liquid. This is something that could be incorporated into the ptychography setup that was initially proposed. Using ptychography to investigate this behaviour is preferable to the confocal microscope due its ability to investigate refractive index shifts and the fact that it has more translational freedom than the confocal microscope. Other experiments could include the expansion of the tests performed in this project to consider the affects of different pH solutions and buffer types, also investigating the affects of different salt concentrations and salt types would offer an interesting experiment to perform. Another system which would be interesting to image would be the semi–critical interfaces such as the one between the liquid system and the boundaries containing the liquid. This could be the cover slide–liquid boundary and the microscope slide–liquid boundary (providing the liquid is sufficiently thin enough that the intensity of the image does not drop off completely).

An interesting observation of the crystals obtained in Figure 18 is their apparent birefringent nature. This is signified by the dark banding in the crystals. The investigation into why this is only seen in some of the crystals and investigations into why the size and shape of the bands vary could also provide a very interesting experiment and is suggested for further experimentation.

5 Conclusion

Through the use of confocal imaging an investigation into the phase behaviour of lysozyme–NaCl solutions has been completed. A successful synthesis method has been created based on the methods proposed by Muschol and Manno [14, 15]. This method has been continually adapted to give a working liquid system that offers consistent behaviour when imaged and responds closely to expected changes in phase. An application method has been developed to reduce the effects of Newtons rings and to ensure the thinnest sample possible. The heating method has been designed around the use of a Peltier heater, which was used to heat the samples through their changes in phase.

To image the liquid behaviour, a script was created for the RDK to operate the microscope through external commands. This script was created to take single slices from the liquid to investigate the behaviour of the liquid at both constant and varying depths. This script was used to collect the intensity data relating to the images produced which was subsequently used to investigate how the intensity of light varies with depth at different temperatures and concentrations of lysozyme. Also an experiment was performed to determine the location of the phase boundary of the lysozyme–NaCl mixtures and experiments were performed to try to investigate the fluctuations of the liquid phases on the boundary between the cloudy and clear phases of the liquid.

It was found that the intensity drops off at a lower distance for solutions in the clear phase, surviving an extra 6–8μm before the intensity was reduced steeply to <50% of the previous intensity. This behaviour was observed in 100mg/ml, 80mg/ml and 60mg/ml lysozyme solutions (in 7% w/v NaCl & 0.1M, pH 5.2 Sodium Acetate buffer solution) which all produced a very similar response. These results are shown on Figure 22 which compares the intensity variations with depth for the cloudy phase and clear phase of the lysozyme–NaCl solutions for the three concentrations tested. This provides evidence of the behaviour that was expected

and also gave a quantitative measure of the difference between the transmission of light through each phase.

Experimentation into the location of the clear to cloudy phase boundary provided results that correlated well with other experimentalists' results. For a 7% w/v solution of NaCl & 0.1M pH 5.2 NaAc buffer solution, the phase boundary was located at $28.65 \pm 0.35\,^{\circ}\mathrm{C}$ (100mg/ml lysozyme), $26.35 \pm 0.45\,^{\circ}\mathrm{C}$ (80mg/ml lysozyme) and $24.55 \pm 0.35\,^{\circ}\mathrm{C}$ (60mg/ml lysozyme). Figure 26 plots these results to a fitted curve given by Equation 1. These results are very similar to the results gained by Muschol and Manno [14, 15] who investigated the same samples (exception being that they used a differing pH of 4.5). The results from this project show a systematic downward shift in temperature compared to Manno and Muschol, which was explained by the use of a differing pH and the errors associated with the reliability of the heating method and the lack of isolation from the liquid's environment.

The solutions were then held at the phase boundary for imaging using the phase boundary values obtained in the previous experimentation, giving unsuccessful results. Using the equipment available, the ability to hold the samples on the phase boundary and to prevent external effects such as evaporation and contamination of the sample was not achievable. Holding the samples in a sealed capillary was also tested in the hope that it would fix the isolation problem. However other unwanted effects started to influence the behaviour of the samples including gravitational separation of the phases and lensing effects which distorted the images produced.

As a result some improvements were suggested including the use of an "oven inside an oven" for more accurate heating and the use of thin square edged capillaries for the isolation issues. But the simplest improvement would be the repeating of the experiments performed which will assess the reliability of the data and should

show up the anomalous results easier.

Also further experimentation was suggested for future investigations including: The use of ptychography to investigate the polarisation and birefringence effects of the liquid, the expansion of the experiment to consider more variables such as salt identity and concentration and buffer identity and pH value, and the investigation of the possible birefringence effects in the cylindrical crystals that were formed (see Figure 18).

References

[1] W. A. Eaton and J. Hofrichter. Sickle cell hemoglobin polymerization. *Advances in Protein Chemistry*, 40:63–279, 1990.

[2] G. G. Glenner. Amyloid deposits and amyloidosis the -fibrilloses. *The New England Journal of Medicine*, 302:1283–1343, 1980.

[3] R. A. Crowther. Structural aspects of pathology in alzheimer's disease. *Biochem. Biophys. Acta.*, 1096:1–9, 1991.

[4] G. Benedek. The molecular basis of cataract formation. *Human Cataract Formation: CIBA Foundation Symposium 106*, pages 237–247, 1984.

[5] C. Gogelein. Phase behaviour of proteins and colloid–polymer mixtures. *Mathematisch–Naturwissenschaftlichen Fakultat der Heinrich–Heine–Universitat Dusseldorf*, 2008.

[6] S. Matsuda, T. Senda, S. Itoh, G. Kawano, M. Mizuno, and Y. Mitsul. New crystal form of recombinant murine interferon–beta. *J. Biol. Chem.*, 264:13381–13382, 1989.

[7] O. Galkin and P. G. Vekilov. Are nucleation kinetics of protein crystals similar to those of liquid droplets? *J. Am. Chem. Soc.*, 122:156–163, 2000.

[8] R. A. Curtis, J. M. Prausnitz, and H. W. Blanch. Protein–protein and protein–salt interactions in aqueous protein solutions containing concentrated electrolytes. *Biotechnol. Bioeng.*, 57:11–21, 1998.

[9] G. A. Manoori. A unified perspective on the phase behaviour of petroleum fluids. *Int. J. Oil, Gas and Coal Technology*, 2(2):141–167, 2009.

[10] A. Kumar, H. R. Krishnamurthy, and E. S. R. Gopal. Equilibrium critical phenomena in binary liquid mixtures. *Physics Reports*, 98(2):57–143, 1983.

[11] E. J. W. Verwey and J. T. G. Overbeek. Theory of the stability of lyophobic colloids. *Dover Publications Inc. New York*, 2000.

[12] F. Cardinaux, T. Gibaud, A. Stradner, and P. Schurtenberger. Interplay between spinodal decomposition and glass formation in proteins exhibiting short–range attractions. *Phys. Rev. Lett.*, 99(11):118301, 2007.

[13] T. Gibaudi. Proteins as model colloids or the physics of dynamical arrest. *phD thesis, University of Freibourg*, 2008.

[14] M. Muschol and F. Rosenberger. Liquid–liquid phase separation in supersaturated lysozyme solutions and associated precipitate formation/crystallization. *J. Chem. Phys.*, 107:1953–1963, 1997.

[15] M. Manno, C. Xiao, D. Bulone, V. Martorana, and P. L. San Biagio. Thermodynamic instability in supersaturated lysozyme solutions: Effect of salt and role of concentration uctuations. *Phys. Rev. E.*, 68:011904, 2003.

[16] N. Wentzel and J. D. Gunton. Liquid–liquid coexistence surface for lysozyme: Role of salt type and salt concentration. *J. Phys. Chem. B*, 111(6):1478–1481, 2007.

[17] Y. Zhang and P. S. Cremer. The inverse and direct hofmeister series for lysozyme. *Proceedings of the National Academy of Sciences*, 106(36):15249–15253, 2009.

[18] J. C. Guillou and J. Zinn-Justin. Critical exponents for the n–vector model in three dimensions from field theory. *Phys. Rev. Lett.*, 39(2):95–98, 1977.

[19] D. C. Phillips. The hen egg white lysozyme molecule. *Proceedings of the National Academy of Sciences of the United States of America*, 57(3):483–495, 1967.

[20] P. J. Cozzone, S. J. Opella, O. Jardetzky, J. Berthou, and P. Jolles. Detection of new temperature–dependent conformational transition in lysozyme by carbon–13 nuclear magnetic resonance spectroscopy. *Proc Natl Acad Sci U S A.*, 72(6):2095–2098., 1975.

[21] C. Muller and J. Ulrich. The dissolution phenomenon of lysozyme crystals. *Cryst. Res. Technol.*, 47(2):169–174, 2012.

[22] P. R. ten Wolde and D. Frenkel. Enhancement of protein crystal nucleation by critical density fluctuations. *Science*, 277:1975–1978, 1997.

[23] V. Ball and J. J. Ramsden. Buffer dependence of refractive index increments of protein solutions. *Biopolymers*, 46:489–492, 1998.

[24] J. Narayanan and X. Y. Liu. Protein interactions in undersaturated and supersaturated solutions: A study using light and x–ray scattering. *Biophysical Journal*, 84:523–532, 2003.

[25] O. D. Velev, E. W. Kaler, and A. M. Lenhoff. Protein interactions in solution characterized by light and neutron scattering: Comparison of lysozyme and chymotrypsinogen. *Biophysical Journal*, 75:2682–2697, 1998.

[26] M. Bostrom, F. W. Tavares, B. W. Ninham, and J. M. Prausnitz. Effect of salt identity on the phase diagram for a globular protein in aqueous electrolyte solution. *J. Phys. Chem. B*, 110:24757–24760, 2006.

[27] Y. X. Huang, G. M. Thurston, D. Blankschtein, and G. B. Benedek. The effect of salt identity and concentration on liquidliquid phase separation in aqueous micellar solutions of c8 lecithin. *J. Chem. Phys*, 92(3):1956–1962, 1990.

[28] V. G. Taratuta, A. Holschbach, G. M. Thurston, D. Blankschtein, and G. B. Benedek. Liquid-liquid phase separation of aqueous lysozyme solutlons: Effects of ph and salt identity. *J. Phys. Chem*, 94:2140–2144, 1990.

[29] J. J. Grigsby, H. W. Blanch, and J. M. Prausnitz. Cloud-point temperatures for lysozyme in electrolyte solutions: effect of salt type, salt concentration and ph. *Biophys. Chem.*, 91:231–243, 2001.

[30] M. C. Heijna, W. J. van Enckevort, and E. Vlieg. Crystal growth in a three-phase system: diffusion and liquid-liquid phase separation in lysozyme crystal growth. *Phys Rev E Stat Nonlin Soft Matter Phys.*, 76:011604, 2007.

[31] M. Lund and P. Jungwirth. Patchy proteins, anions and the hofmeister series. *J. Phys. Condens. Matter*, 20:494218, 2008.

[32] M. Bostrom, D. R. M. Williams, and B. W. Ninham. Specific ion effects: Why the properties of lysozyme in salt solutions follow a hofmeister series. *Biophys J.*, 85(2):686–694, 2003.

[33] R. H. Webb. Confocal optical microscopy. *Rep. Prog. Phys.*, 59:427–471, 1996.

[34] Hampton Research. hr002676 new user guide. 2012.

[35] Y. Vasylkiv, Y. Nastishin, and R. Vlokh. On the problem of phase transitions in lysozyme crystals. *Institute of Physical Optics, Ukraine*, 2007.

6 Appendix

6.1 Heating System – Temperature Dependence Graphs

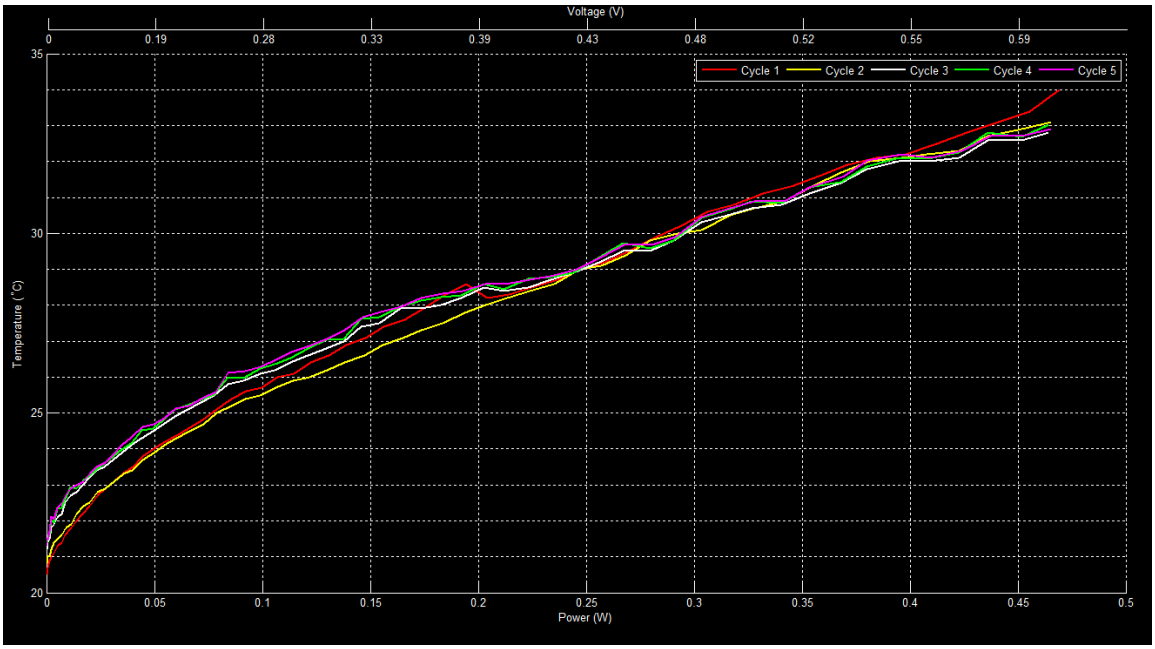

Figure 6: This figure describes the temperature dependence of the peltier heaters as a function of power for five cycles. There was a waiting period of 20 seconds between each data point and a 10 minute wait between each cycle.

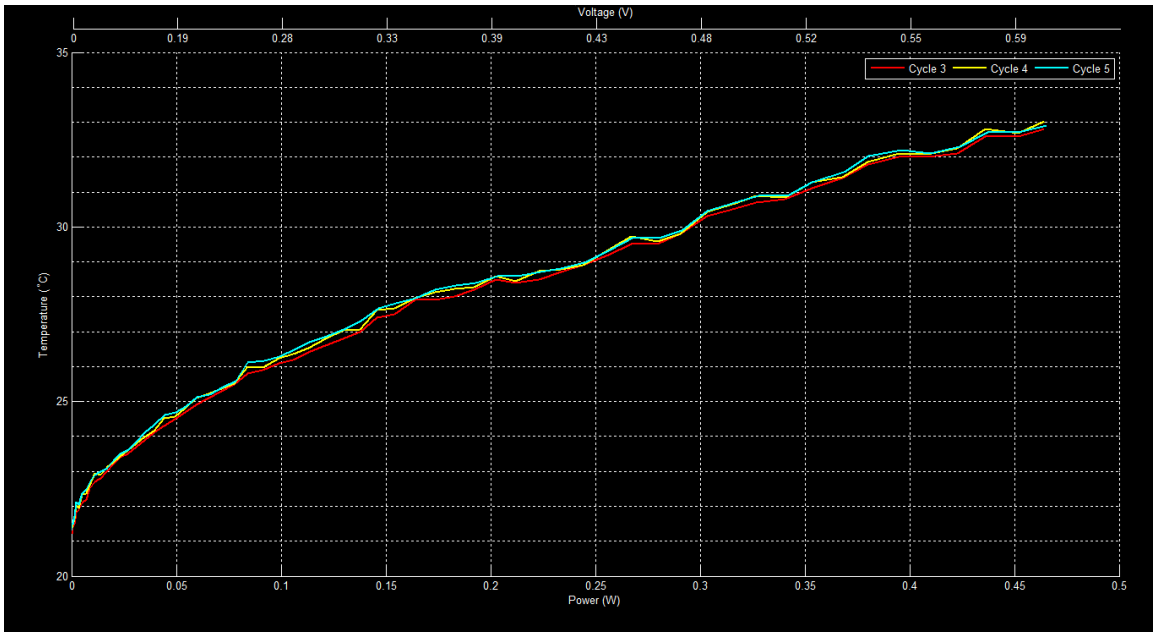

Figure 7: This figure describes the temperature dependence of the peltier heaters as a function of power focusing on the last three "stable" cycles. Again, there was a waiting period of 20 seconds between each data point and a 10 minute wait between each cycle.

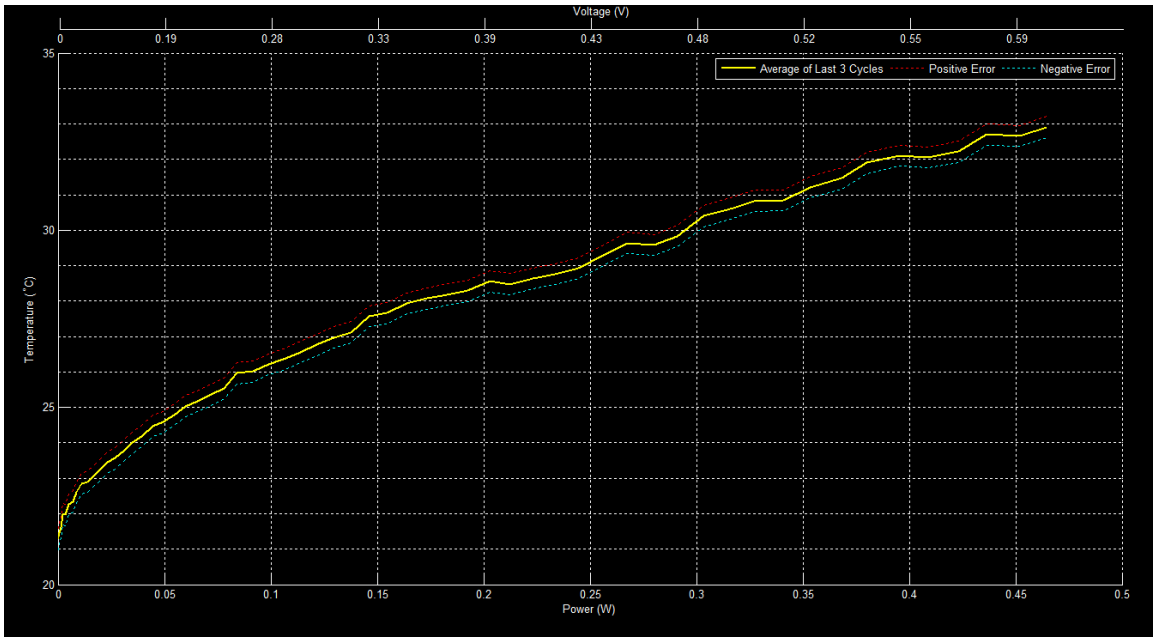

Figure 8: This figure describes the average temperature dependence of the peltier heaters as a function of power when only the last three "stable" cycles are taken into consideration. There was a waiting period of 20 seconds between each data point and a 10 minute wait between each cycle. The positive and negative errors are given by the largest range between the temperature recordings in the last three cycles. This difference was 0.3 °C.

6.2 Script Files

6.2.1 Z–Stacking Script

The following script was designed to create slices using the LEXT software package with the OLS4000 Confocal Microscope. It was created using the text editing software notepad, but can be used with any similar word processing software (ensuring that scripts are saved with the .txt extension) and was designed for use on the RDK for the LEXT software. At first you must configure the host computer (the one connected to the confocal microscope) and the user computer (the computer where the RDK is installed). Once connected, the RDK application can be used to send commands through the connecting interface to the host computer. This allows the operation of the microscope to be determined remotely and for the imaging to be customised to the user's needs without having to rely on presets.

The sample code below includes a short passage describing the purpose of each line of code and is included to help with the understanding of the script. Please refer to the RDK user guide offered by Olympus for a full breakdown of codes, troubleshooting and information on how to connect the user and host computers.

Note, the double back space in the following script allows for comments to be shown but tells the RDK to ignore them. So if you use this code with the RDK it will work regardless of the comments made.

Note, in this script shown, it refers to the use of a "wizard". This wizard consists of a simple code that is designed to create a .tif of the resultant slice. This image can be created using the LEXT software, by clicking on the measurement tab and then subsequently on the wizard tab. This will bring up a box on the bottom right hand side of the screen, in here you will need to right click and select from the options "export image...". There will then be a new box opened which will lead you through the setup of the exporting function. Select .tiff as the exporting file type and set a path for the resultant images. Save this wizard and then call it within the RDK script by entering the name of the saved wizard after the "RDWIZ= " command.

```
[OLS4000 Ver2.1 RDK Script.]
//This must be placed at the top of every script the user creates
CONNECT= 0
//Connects to the host computer
INITNRML= "Insert Username","Insert Password"
//Starts up the LEXT software and logs into the account as entered - Useful as the
//software will load the default settings for the account, preserving auto save
features
// and shot mode etc...
//If the user does not have the correct start up settings required then a
configuration
// file which contains all of the settings required (which contains many settings
such
// as the shot mode, default lens and zoom etc...) can be saved by the user (under
the
// advanced settings tab) and can be linked to in this script by using the command:
//RDSETTING= 0,PATH
//Where path denotes the location of the file. E.G.
c:/Desktop/ConfigurationFile.acd
[Wait= 1000]
//Wait Function is in Milliseconds and is included here to prevent problems from
sending
// the codes below before the software has fully initialised (as a fail-safe)
CHMODE= 1
//This Function locks the software to only accept commands from this script
LIVE= 1,1
//This initiates the laser acquisition mode and the live view on the screen
CHOB= 6
//This changes the objective to the 6th lens. 1=2.5x, 2=5x, 3=10x, 4=20x, 5=50x,
6=100x
MVZHOME= 0
//This moves the focal plane to the origin position (Z=0)
MVZR= 40
//The idea behind this slicing method is that before this script is run the user
positions
// the focal point origin at the top of the sample using the manual controls on the
side
// of the microscope. But this is not always possible when using the higher
magnification
// lenses as the small changes required to move it in position are almost
impossible to
// do manually. The user is advised to find roughly the top of the sample (with the
lens
// at the origin focal point) and then move the lens using the software to make
these
// small adjustments. The user should then take note of the depth position given by
the
// software (at the bottom of the image). This command moves the lens to this
position,
// so that the slicing begins from the top of the sample. If the user manages to
find the
// top of the sample using the manual methods this command can be deleted (or the
number
// set to 0). The command moves the focal point down for positive numbers and up
for
// negative numbers.
[WAIT= 5000]
//This wait function is added to allow for the software to recover from
oversaturation
// which may occur as a result of moving to the new position. Without this, the
software
// hangs whilst it reduces the brightness and may skip the next line of code
(usually
// leaving the user with a blank image).
AEEXE= 1
//This executes the auto exposure function to adjust the brightness of the sample.
CHATSAVE= 1,"PATH","NAME YOU WANT TO ASSIGN THE SAVED DATA WITH","NUMBER WHERE YOU
WANT THE AUTO NUMBERING TO START"
```

```
//This Function configures the auto save feature so that all files are saved in the
PATH
// specified by the user above. Each file is then given a name and a number
relating to
// the slice number.
SHOT= 0
//This function initiates acquisition. (For slicing the user must ensure that the
// snapshot mode is saved as a default on their account or that snapshot mode is
included
// in the configuration file).
RDWIZ= Save as TIFF and CSV in holding folder
//This loads a wizard called "Save as TIFF and CSV in holding folder" which saves a
TIFF
// of the Slice. This wizard was created by me and so it saves the TIFF into a
folder which
// is set when the wizard is created. You will need to create your own for this, i
can
// show you how to do it if you need me to.
WIZEXE= 0
//This function initiates the wizard.
ENDWIZ= 0
//This function ends the wizard.
QUITWIZ= 0
//This function quits the wizard.
//The codes below then perform the slicing (note each slice moves down by 4
micrometers).
// It starts from the position as set from the above settings and saves all files
into the
// path as the name and number of slice as entered above.
Loop n
//This command loops the following commands that are between "loop n" and "loopend"
"n" times
CHMODE= 1
LIVE= 1,1
[Wait= 5000]
AEEXE= 1
MVZR= 4
SHOT= 0
RDWIZ= Save as TIFF and CSV in holding folder
WIZEXE= 0
ENDWIZ= 0
QUITWIZ= 0
Loopend
//This command sets the end of the loop sequence as explained above
[Wait= 120000]
//This wait function is for my use to allow for me to change the voltage manually
before the slicing begins again
//this whole process can then be looped again using the loop and loopend functions
so that
//once the voltage has been changed and after the 120000 wait function, the slicing
//will begin again (although please remember to set the save folder as something
else to
//prevent overwriting previous data! - this happened a lot in this project..)
```

6.2.2 VBA .csv Importing Script

```
'This code below describes how the .csv files are imported as seperate
sheets in the New Blank worksheet

Sub Example12()

Dim MyPath As String

Dim FilesInPath As String

Dim MyFiles() As String

Dim SourceRcount As Long

Dim Fnum As Long

Dim mybook As Workbook

Dim basebook As Workbook

'These commands declare the variables used in the rest of the code

Sheets("Sheet1").Name = "OverallIntensity"

Range("B5").Select

ActiveCell.FormulaR1C1 = "Sheet Name"

Range("C5").Select

ActiveCell.FormulaR1C1 = "Sum"

Range("D5").Select

ActiveCell.FormulaR1C1 = "Average"

'These series of codes above will change the blank workbook so that Sheet1
is renamed OverallIntensity and contains three collums labelled Sheet Name,
Sum and Average (which will later contain the sheet name's Total
(sum)intensity and average intensity)

MyPath = "PATH TO THE FOLDER IN WHICH THE .CSV FILES ARE LOCATED"

'Insert the path to the folder which contains the .csv files

'The below code converts each .csv file in the folder selected to displayed
data in a new sheet within the workbook. The name of each sheet is given by
the .csv file that was imported and contains all of the data from the .csv
within it.

If Right(MyPath, 1) <> "\" Then

MyPath = MyPath & "\"

End If

FilesInPath = Dir(MyPath & "*.csv")

If FilesInPath = "" Then

MsgBox "No files found"

Exit Sub

End If
```

```
On Error GoTo CleanUp
Application.ScreenUpdating = False
Set basebook = ThisWorkbook
Fnum = 0
Do While FilesInPath <> ""
Fnum = Fnum + 1
ReDim Preserve MyFiles(1 To Fnum)
MyFiles(Fnum) = FilesInPath
FilesInPath = Dir()
Loop
If Fnum > 0 Then
For Fnum = LBound(MyFiles) To UBound(MyFiles)
Set mybook = Workbooks.Open(MyPath & MyFiles(Fnum))
mybook.Worksheets(1).Copy After:= _
basebook.Sheets(basebook.Sheets.Count)
On Error Resume Next
ActiveSheet.Name = mybook.Name
On Error GoTo 0
mybook.Close savechanges:=False
Next Fnum
End If
CleanUp:
Application.ScreenUpdating = True
End Sub
'The next script below calculates the average and total intensities and
then puts them in a table Located at F3:H3 underneath headings describing
the relevant data.
Sub AverageSum()
  Dim Sheet As Worksheet


 Sheets("OverallIntensity").Select
  Do
        Range("F2").Select
        ActiveCell.FormulaR1C1 = "Sheet Name"
```

```
        Range("G2").Select
        ActiveCell.FormulaR1C1 = "Sum"
        Range("H2").Select
        ActiveCell.FormulaR1C1 = "Average"
        Range("F3").Select
        ActiveCell.FormulaR1C1 = "=R[-1]C[-5]"
        Range("G3").Select
        ActiveCell.FormulaR1C1 = "=SUM(R[13]C[-5]:R[1036]C[506])"
        Range("H3").Select
        ActiveCell.FormulaR1C1 = "=AVERAGE(R[13]C[-6]:R[1036]C[505])"


    Range("F3:H3").Select
    Selection.Copy
    Range("F4").Select
    Selection.PasteSpecial Paste:=xlPasteValues, _
    Operation:=xlNone, SkipBlanks:=False, Transpose:=False
    Range("F3").Select
    Application.CutCopyMode = False
    Columns("F:H").Select
    Selection.Columns.AutoFit
    Worksheets(ActiveSheet.Index + 1).Select
Loop
End Sub

'The script below will delete Sheet2 and Sheet3 which are empty and not
needed. It also coppies and pastes the Sum, Average and Sheet Name data
from each consecutive sheet onto a new row underneath the headings (sheet
name, average and sum) on the OverallIntensity sheet (the ones that we
created in the first script).



Sub CopyIt()
    Dim Sheet As Worksheet
    Application.ScreenUpdating = False
    Sheets("OverallIntensity").Select
    For Each Sheet In ActiveWorkbook.Worksheets
```

```
        If Sheet.Name <> "OverallIntensity" Then

            Sheet.Range("F4:H4").Copy
Sheets("OverallIntensity").Cells(Rows.Count, "B").End(xlUp).Offset(1)

        End If

    Next

    Application.ScreenUpdating = True

    Columns("B:D").Select

            Selection.Columns.AutoFit

            Sheets("OverallIntensity").Select

    Range("F2:H4").Select

    Selection.ClearContents

    Sheets("Sheet2").Select

    ActiveWindow.SelectedSheets.Delete

    Sheets("Sheet3").Select

    ActiveWindow.SelectedSheets.Delete

    Sheets("OverallIntensity").Select

    Range("B6:D7").Select

    Selection.ClearContents

    Range("B5:D5").Select

    Selection.Cut Destination:=Range("B7:D7")

    Range("B7:D7").Select

End Sub

'Note, i have decided to not compile all three scripts into one big script
for the sake of risking errors. It also allows me to only run the scripts
for the data that i wish to create as computational time can be lengthy
when using lots of .csv files. This means that i do not waste unnecessary
time waiting for data that i do not need. This code serves as a basis for
the codes used. If other data was required to be analysed then i would
insert the correct command into one of the above scripts. E.g. if one
wanted to work out the median or range of intensities or if you wanted to
insert a code to account for background then that can be added easily using
the above scripts as a basis.
```

6.2.3 Intensity vs Slice Number Graphing Codes

%Data was imported from the .csv files using the VBA script (named c100mg,c80mg and c60mg) and then they were imported into matlab and split into sections describing each voltage (instead of a large continuous set of data, it was split into separate cells with each cell containing data for each voltage (temperature) reading). This was done using the code below:

```
A=mat2cell(c100mg,18*ones(15,1),2);
A2=mat2cell(c80mg,18*ones(15,1),2);
A3=mat2cell(c60mg,18*ones(15,1),2);
%A=100 mg data, A2=80mg data and A3=60mg data.
%The array according to the voltage section can then be called upon using the A{i} code where i is the number of the voltage reading (For the first set of data in the excel document e.g. 0.36V for 100mg, i=1 and the last has i=15 - as there were 15 voltages tested).
%This code below describes how the graphs were created to allow for the intensity vs slice number graphs.
mpdc10 = distinguishable_colors(20);
ha = axes; hold(ha,'on')
set(ha,'ColorOrder',mpdc10)
hold all
for i=1:15;
plot(A{i}(:,2),A{i}(:,1));
end
Legend=cell(15,1);
for iter=1:15;
Legend{iter}=strcat('Data Set Number ', num2str(iter));
end
legend(Legend,'Location','NorthWest')
title('Intensity Variations vs Slice Depth for a 100mg/ml Lysozyme Solution (Voltages Start at 0.36V, With Increments of 0.01V for Each Data Set)')
xlabel('Slice Number')
ylabel('Intensity (Arbitrary Units)')
hold off
figure
hold all
for i=1:6
plot(A{i}(:,2),A{i}(:,1));
end
Legend=cell(6,1);
for iter=1:6;
Legend{iter}=strcat('Data Set Number ', num2str(iter));
end
legend(Legend,'Location','NorthWest')
title('Intensity Variations vs Slice Depth for a 100mg/ml Lysozyme Solution - Before the Phase Separation - (Voltages Start at 0.36V, With Increments of 0.01V for Each Data Set)')
```

```
xlabel('Slice Number')
ylabel('Intensity (Arbitrary Units)')
hold off
figure
hold all
for i=7:15
plot(A{i}(:,2),A{i}(:,1));
end
Legend=cell(15,1);
for iter=1:15;
Legend{iter}=strcat('Data Set Number ', num2str(iter));
end
legend(Legend,'Location','NorthWest')
title('Intensity Variations vs Slice Depth for a 100mg/ml Lysozyme Solution
- After the Phase Separation - (Voltages Start at 0.42V, With Increments of
0.01V for Each Data Set)')
xlabel('Slice Number')
ylabel('Intensity (Arbitrary Units)')
hold off
figure

%As the only data for the 80mg and 60mg solutions were slices for a cloudy
phase and slices for the clear phase, a graph was created to compare the
intensity variations of these phases for the 60mg, 80mg and 100mg samples
this was done using the graph below:

hold all
plot(A{1}(:,2),A{1}(:,1))
plot(A{15}(:,2),A{15}(:,1))
plot(A2{1}(:,2),A2{1}(:,1))
plot(A2{15}(:,2),A2{15}(:,1))
plot(A3{1}(:,2),A3{1}(:,1))
plot(A3{15}(:,2),A3{15}(:,1))
legend('100mg/ml 0.36V','100mg/ml 0.50V','80mg/ml 0.23V','80mg/ml
0.37V','60mg/ml 0.13V','60mg/ml 0.27V','Location','NorthWest')
title('Intensity Variations With Depth for 100mg/ml, 80mg/ml and 60mg/ml
samples - Comparing Only the Lowest and Highest Temperatures Used (Cloudy
and Non-Cloudy Phases)')
xlabel('Slice Number')
ylabel('Intensity (Arbitrary Units)')
hold off
```

6.2.4 Fitting to Experimental Values Graphing Codes

The graphs showing the phase boundary results of this experiment, Muschol et al. [14] and Manno et al. [15] (Figure 26, Page 96) were created by fitting the data to Equation 1 using a least squares method on the equation with $c_{crit} = 255$ and variables T and A, using an exponent of 0.325 [14, 18]. The code for accomplishing this is displayed below.

```
A=[0:0.1:1000];
T=[0:0.1:1000];
% Initialize arrays to store fits and goodness-of-fit.
fitresult = cell( 3, 1 );
gof = struct( 'sse', cell( 3, 1 ), ...
'rsquare', [], 'dfe', [], 'adjrsquare', [], 'rmse', [] );
%% Fit: 'untitled fit 1'.
% This is the fit for Muschol’s data
[xData, yData] = prepareCurveData( CMU, TMU );
% Set up fittype and options.
ft = fittype( 'AT-Ac*((255-x)/255)^(1/0.325)', 'independent', 'x',
'dependent', 'y' );
opts = fitoptions( 'Method', 'NonlinearLeastSquares' );
opts.Display = 'Off';
opts.StartPoint = [0.438744359656398 0.381558457093008];
% Fit model to data.
[fitresult{1}, gof(1)] = fit( xData, yData, ft, opts );
% Plot fit with data.
figure( 'Name', 'untitled fit 1' );
h = plot( fitresult{1}, xData, yData );
legend( h, 'TMU vs. CMU', 'untitled fit 1', 'Location', 'NorthEast' );
% Label axes
xlabel( 'CMU' );
ylabel( 'TMU' );
grid on
%% Fit: 'untitled fit 2'.
% This is the fit for Manno’s data
[xData, yData] = prepareCurveData( CMA, TMA );
% Set up fittype and options.
```

```
ft = fittype( 'AT-A*((255-x)/255)^(1/0.325)', 'independent', 'x',
'dependent', 'y' );
opts = fitoptions( 'Method', 'NonlinearLeastSquares' );
opts.Display = 'Off';
opts.StartPoint = [0.0344460805029088 0.950222048838355];
% Fit model to data.
[fitresult{2}, gof(2)] = fit( xData, yData, ft, opts );
% Plot fit with data.
figure( 'Name', 'untitled fit 2' );
h = plot( fitresult{2}, xData, yData );
legend( h, 'TMA vs. CMA', 'untitled fit 2', 'Location', 'NorthEast' );
% Label axes
xlabel( 'CMA' );
ylabel( 'TMA' );
grid on
%% Fit: 'untitled fit 3'.
% This is the fit for this experiments data
[xData, yData] = prepareCurveData( CME, TME );
% Set up fittype and options.
ft = fittype( 'AT-A*((255-x)/255)^(1/0.325)', 'independent', 'x',
'dependent', 'y' );
opts = fitoptions( 'Method', 'NonlinearLeastSquares' );
opts.Display = 'Off';
opts.StartPoint = [0.317099480060861 0.694828622975817];
% Fit model to data.
[fitresult{3}, gof(3)] = fit( xData, yData, ft, opts );
% Plot fit with data.
figure( 'Name', 'untitled fit 3' );
h = plot( fitresult{3}, xData, yData );
legend( h, 'TME vs. CME', 'untitled fit 3', 'Location', 'NorthEast' );
% Label axes
```

```
xlabel( 'CME' );
ylabel( 'TME' );
grid on
```

The fitted data was then saved under FitMu, (fit for Muschol et al.) FitMa, (fit for Manno et al.) and FitMe (for the experimental data in this project).

Then it was plotted onto a graph that plots Muschol's, Manno's and this experiments work.

This was done by utilising thee "hold on" and plot(x,y) functions and then formatting the resultant graph to look clearer.

6.3 Experimental Images and Data

6.3.1 Initial Experimentation – Images and Data

Figure 9: This image show what the software produced when imaging uing the continuous scanning mode. When there is no solid structure in the liquid, the software identifies the cover slide as the focal point of the imaging.

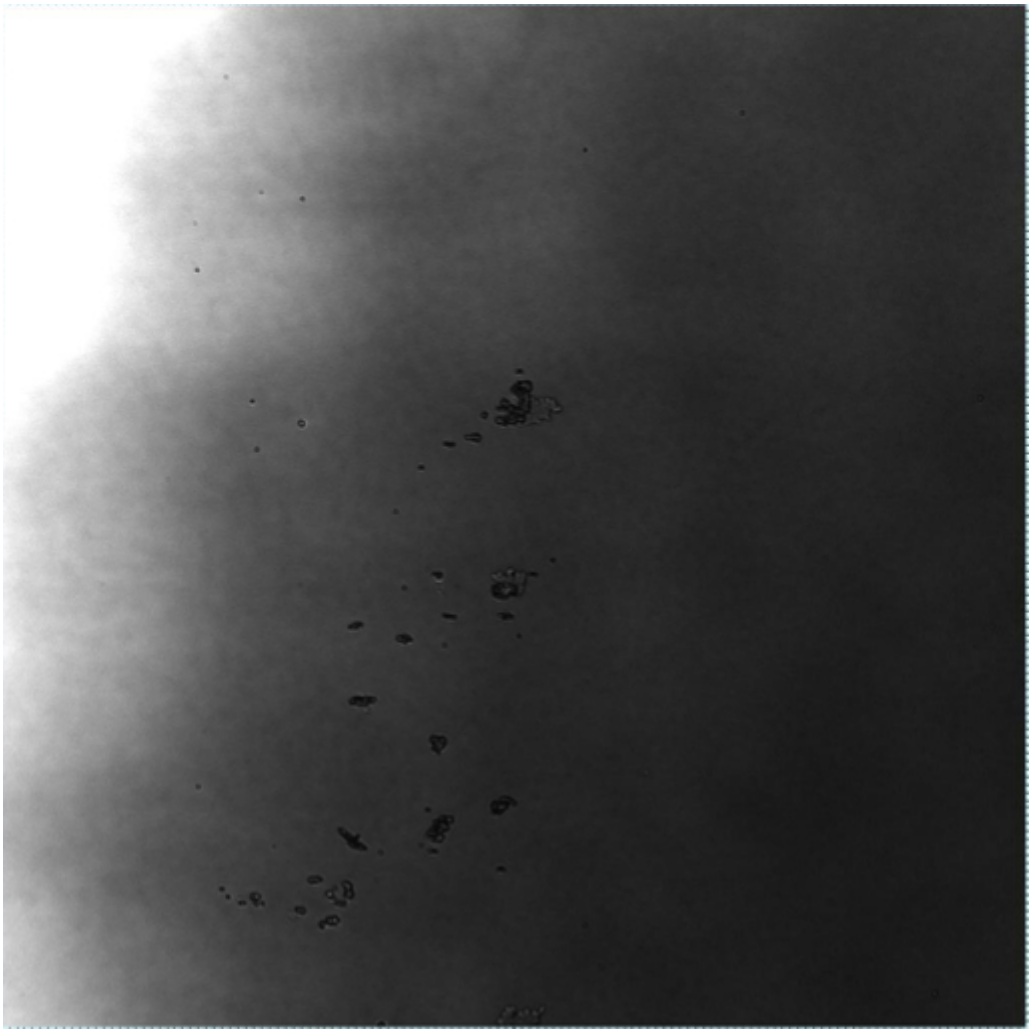

Figure 10: This image is another example of what is produced when imaging using the continuous scanning mode on the liquid samples. Like before, the software has focussed onto the cover slide and not the liquid sample.

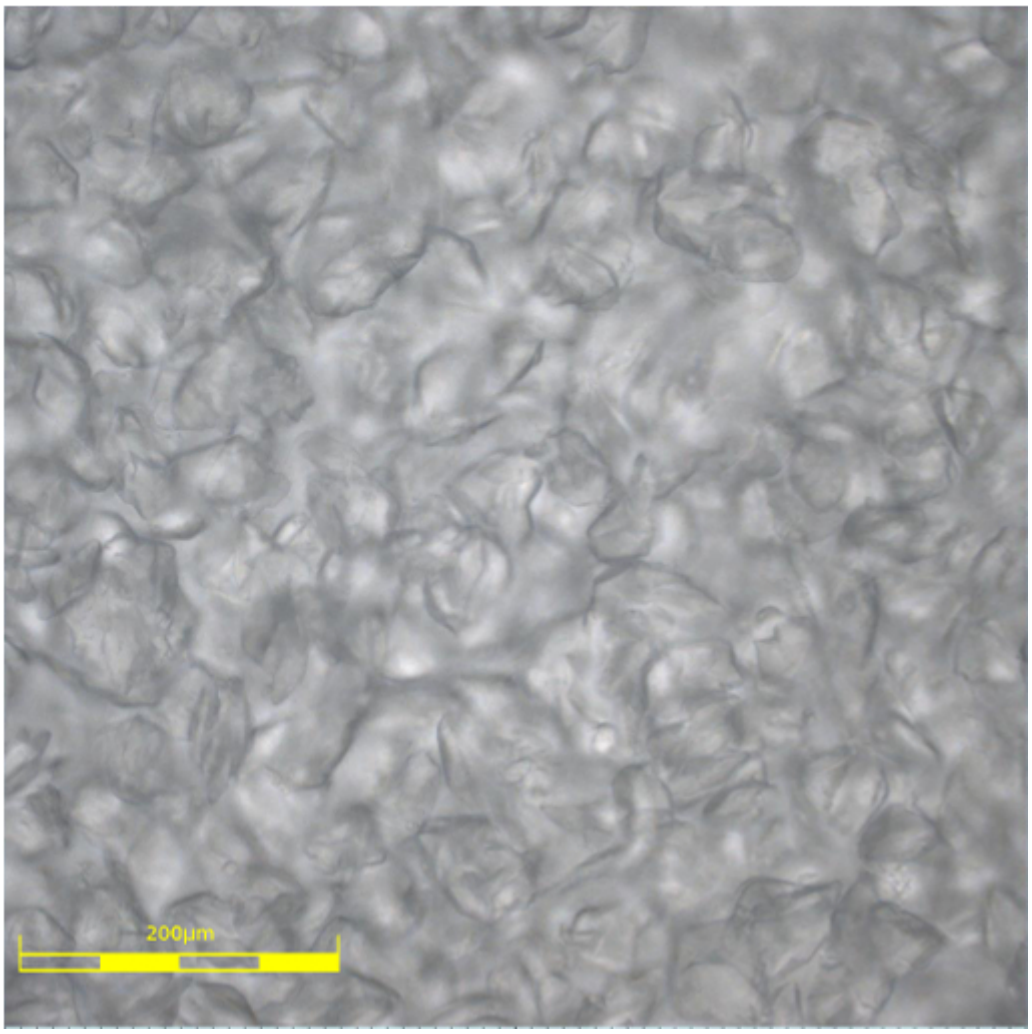

Figure 11: This colour image shows the crystal formation that was observed in the dense lower area of a 176mg/ml lysozyme, 7% w/v NaCl and 1ml, 0.1M NaAc solution. Note that the scale is different to Figure 12 and is only imaged under 20x magnification.

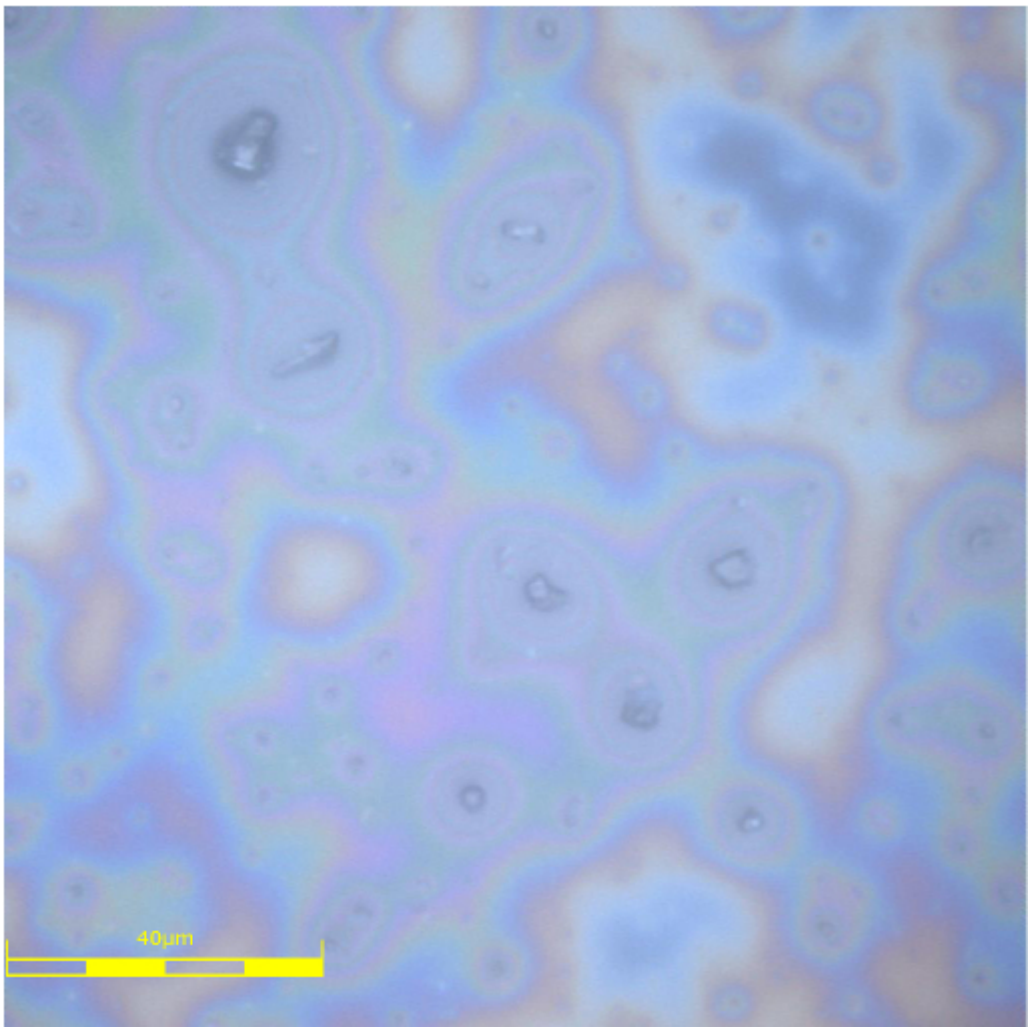

Figure 12: This colour image shows the crystal formation that was observed in the more sparse upper area of a 176mg/ml lysozyme, 7% w/v NaCl and 1ml, 0.1M NaAc solution. Note that the scale is different to Figure 11 and is only imaged under 100x magnification. It is clear that there is a huge difference between the sizes of the crystals in this sample and compared to Figure 11.

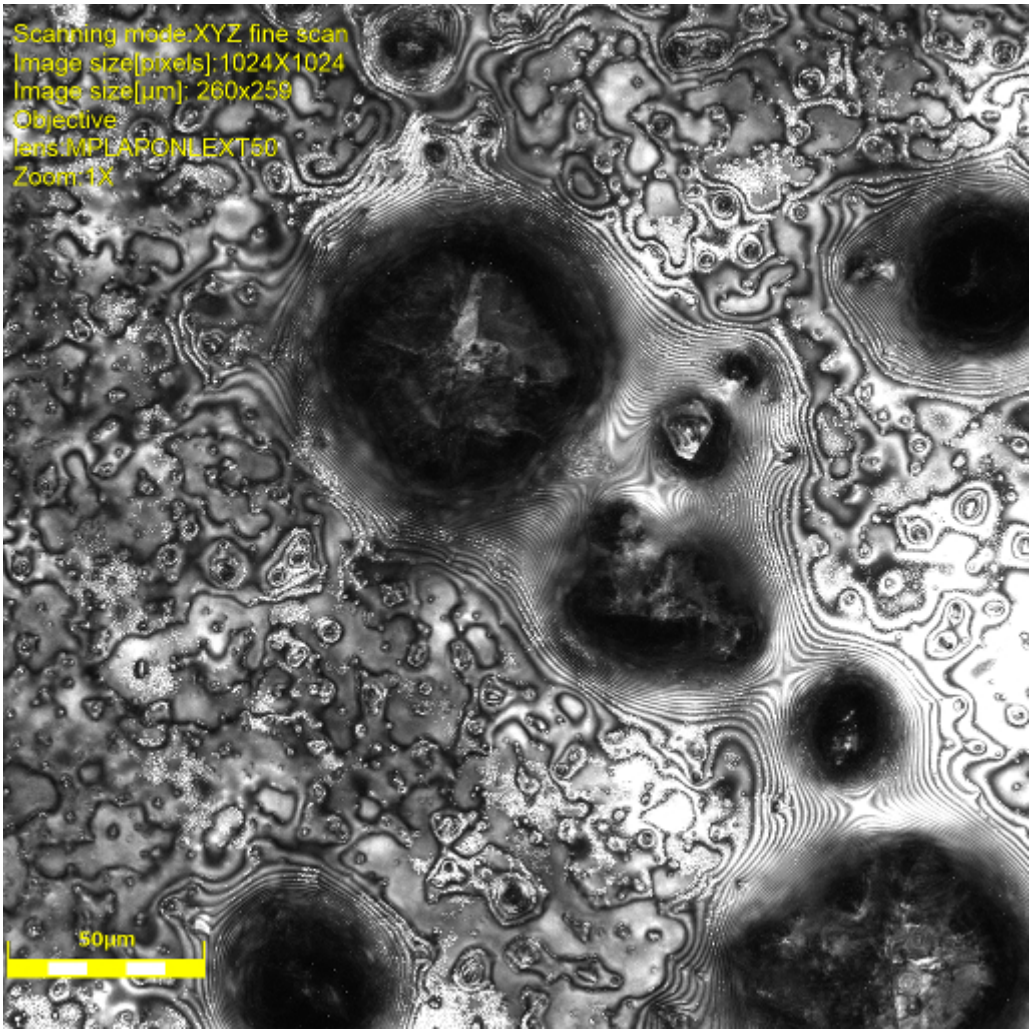

Figure 13: This LASER image shows a single crystal found within the same sample as in Figure 11. As you can see, the crystal has adopted the tetragonal structure. Imaged under 50x magnification.

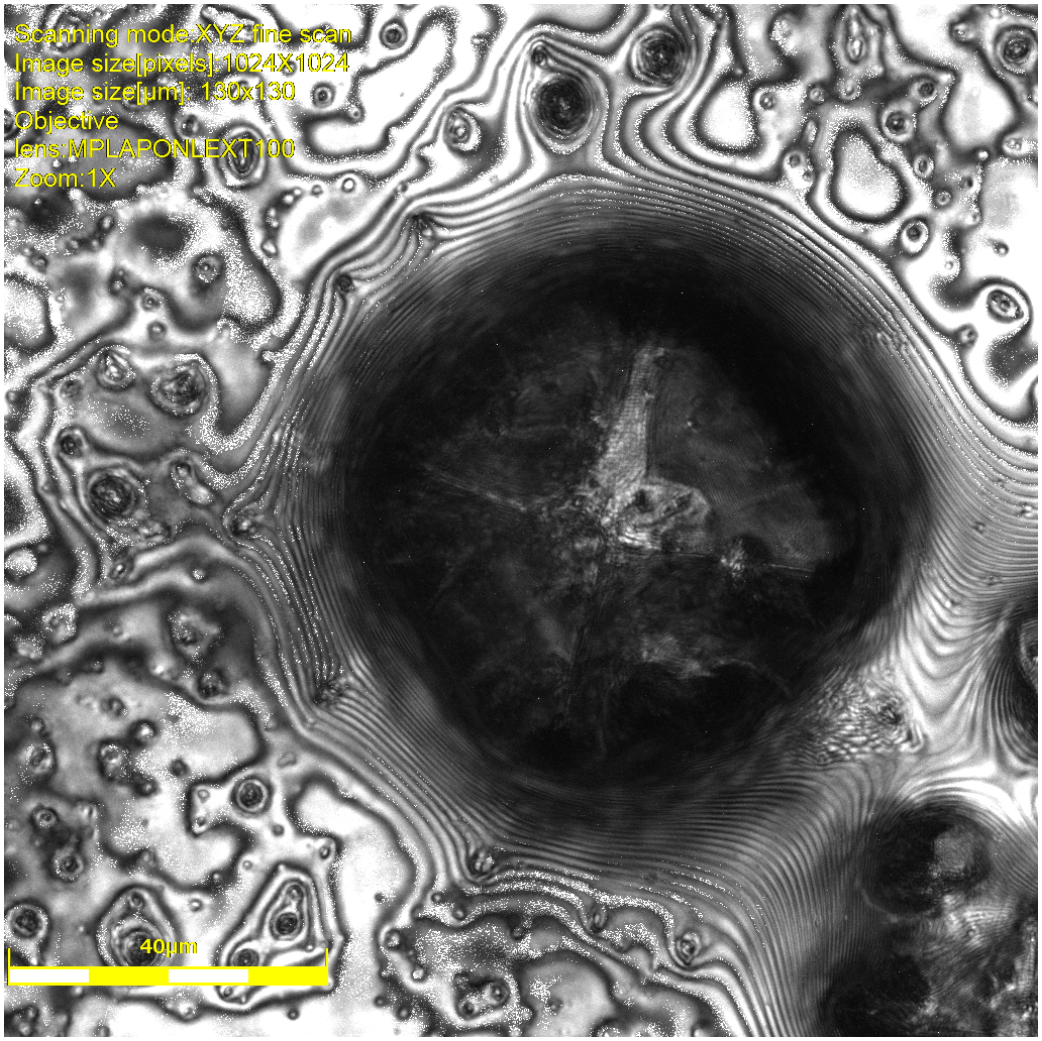

Figure 14: This LASER image shows a more enlarged version of Figure 13 to show more clearly the tetragonal structure. It is roughly 55–60μm in diameter. Imaged under 100x magnification.

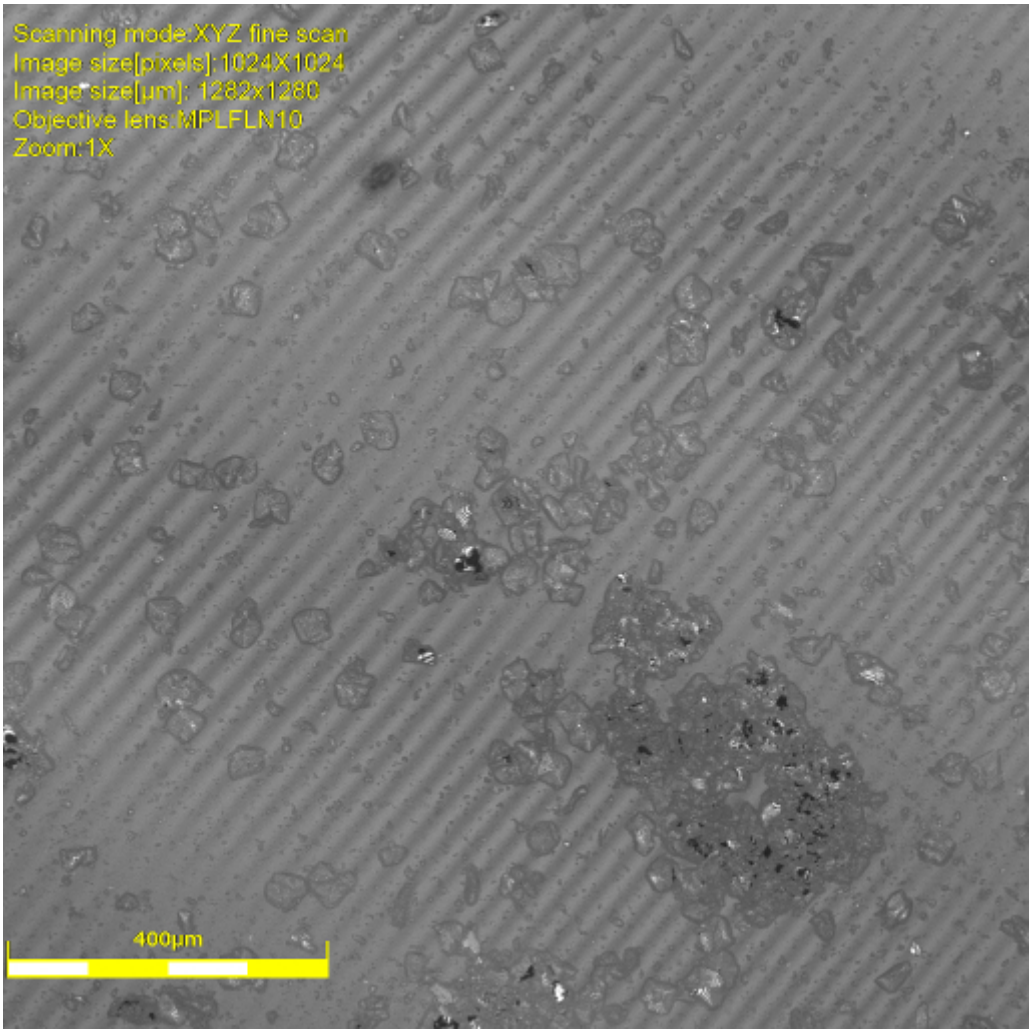

Figure 15: This LASER image shows the same sample as in Figure 12 and Figure 11. This sample was gently vortexed to mix the two crystal sizes resulting in a variety of shapes and sizes of crystals. However, this change in shape and size is most likely down to collisional break up of the crystals. Imaged under 10x magnification.

6.3.2 Final Experimentation – Images and Data

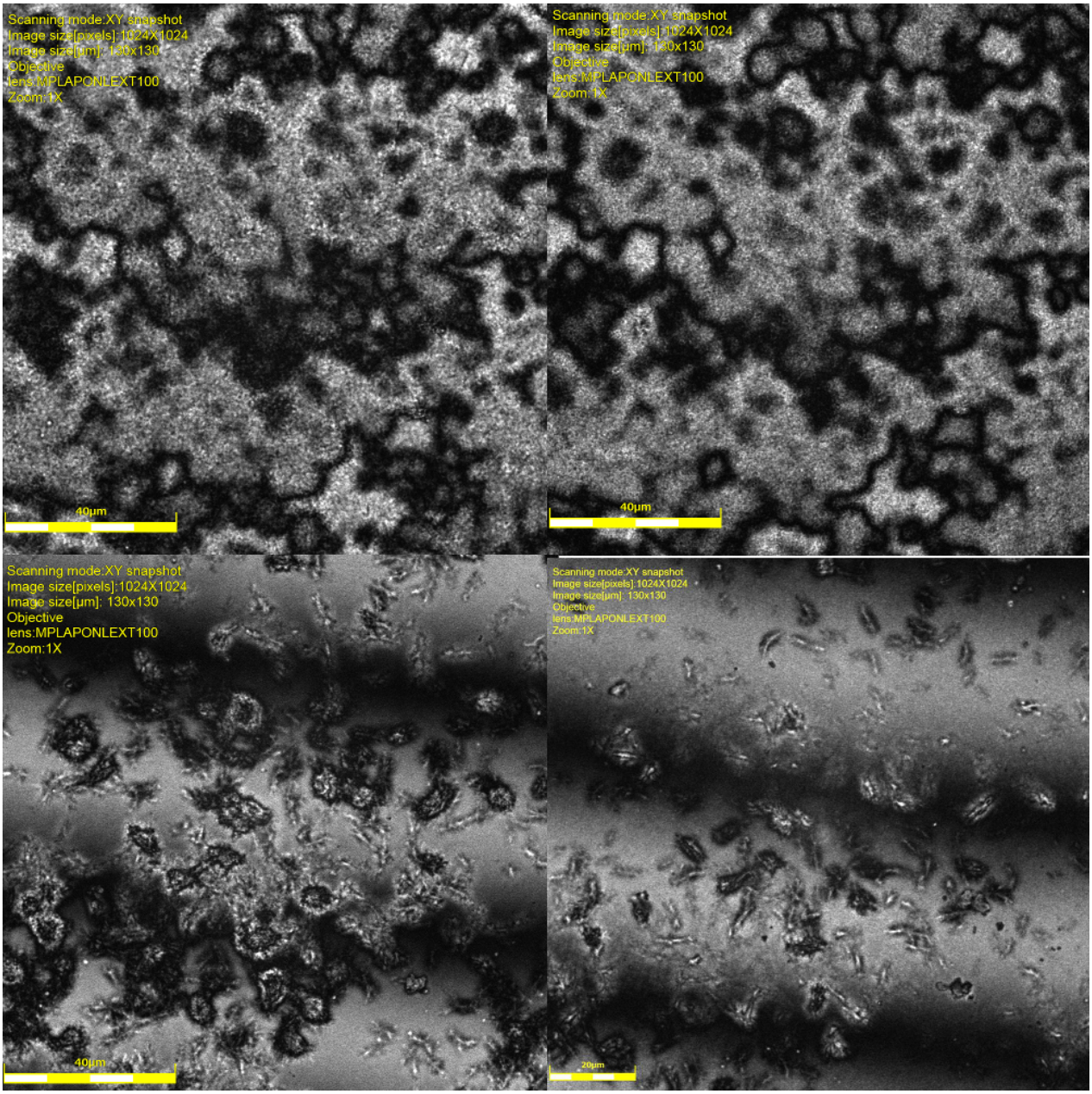

Figure 16: This figure shows some of the constant temperature slices of a 100mg/ml lysozyme solution when held on the phase boundary. Unfortunately the precise location of the phase boundary was not replicable and resulted in the image either being in the cloudy phase (top two images) or just above the phase boundary (bottom two images). No images were obtainable of the exact phase boundary temperature.

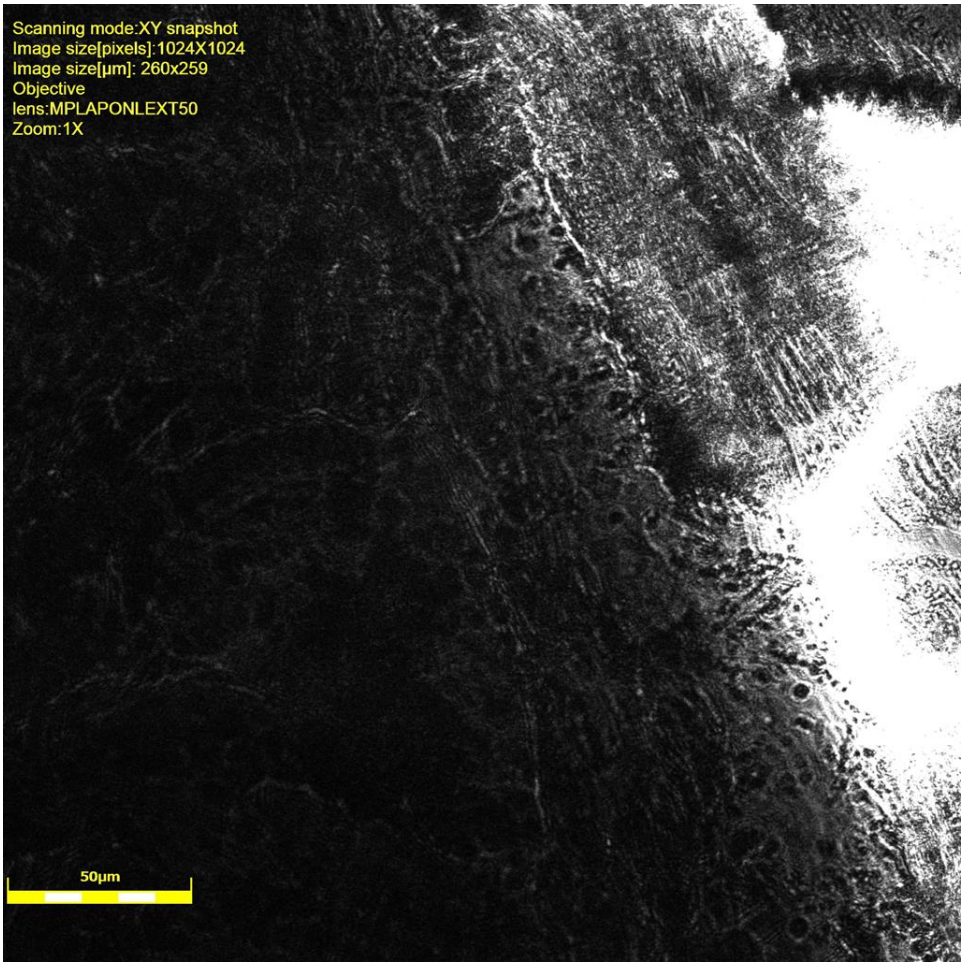

Figure 17: This image shows an attempt at using the continuous scanning mode to image the samples. The software appears to have focussed on only the top/bottom of the sample and not the liquid sample.

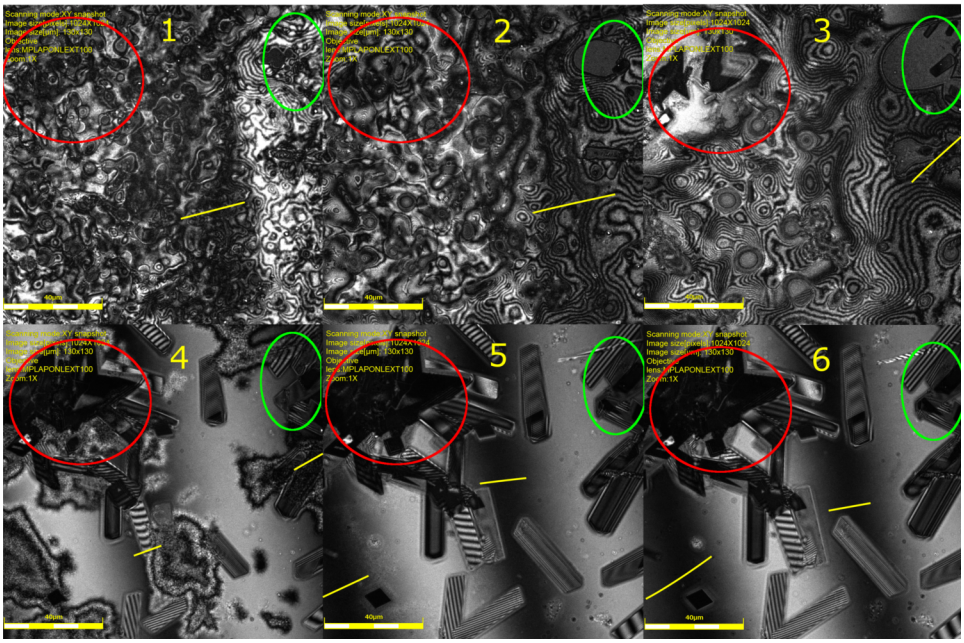

Figure 18: This image shows a series of slices taken form a sample of 100mg/ml lysozyme in 7% w/v NaCl solution of 0.1M, pH 5.2 NaAc. The images were taken one hour apart at a Peltier voltage supply increasing by 2V with each image. They are all of the same depth within the sample. Image 1 starts at t=0 and 36V. The green circle shows an area of the sample where crystal formation is occurring. The red circle shows crystal formation and in image four it is easy to see that the crystal growth is only occurring in areas of the high density phase. The crystals grow at different rates at different times (probably indicative of the different temperatures, crystal surface areas and lysozyme concentrations in each image), this rate slows down significantly in image 6 and is likely due to the available lysozyme being exhausted. Note, the crystals start to become visible after about three hours. This indicates that crystal growth alters the local lysozyme concentration near to where the crystal is forming. The yellow lines indicate regions of low intensity caused by interference effects in the cover slide. these bands are next to high intensity bands and signify the Newtons rings effect. Also, note the banded structure of some of the crystals, this could be evidence for the birefringent nature of lysozyme crystals which could provide an interesting experiment if the investigation of this behaviour was performed.

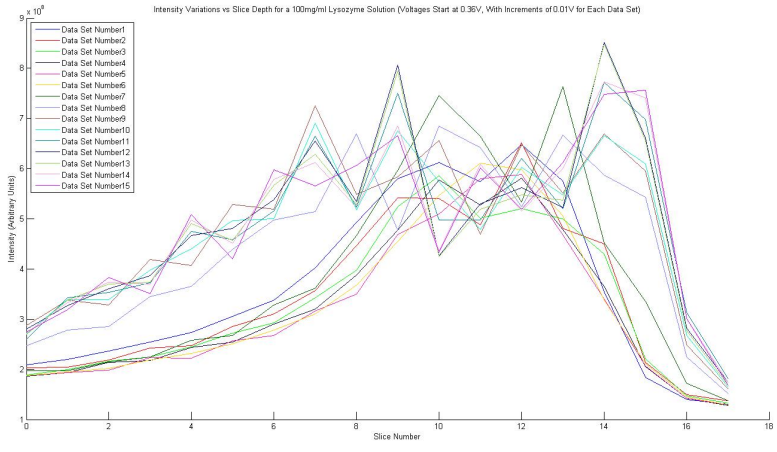

Figure 19: This image shows how the intensity varies with depth in a 100mg/ml lysozyme solution. Each slice is separated by 2μm.

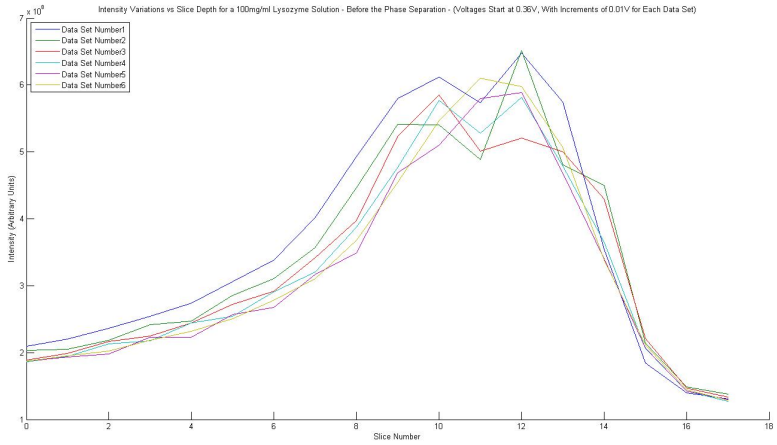

Figure 20: This image shows how the intensity varies with depth in a 100mg/ml lysozyme solution, considering only the cloudy point data (all Voltages/Temps that cause the cloudy phase). Each slice is separated by 2μm.

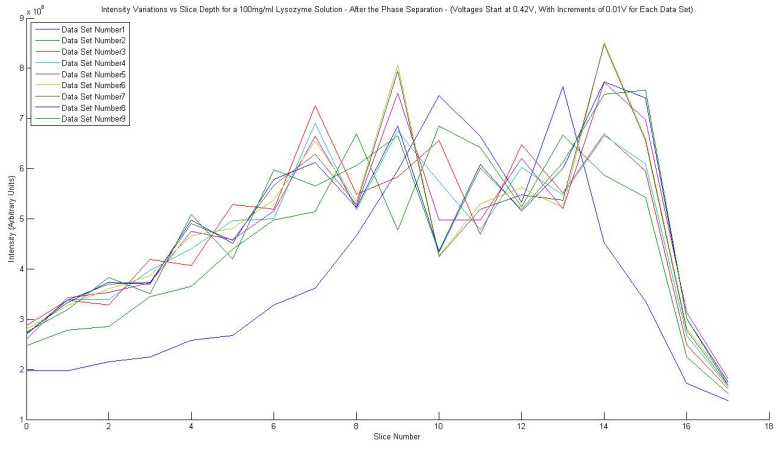

Figure 21: This image shows how the intensity varies with depth in a 100mg/ml lysozyme solution, considering only the non cloudy point data (all Voltages/Temps that cause the clear phase). Each slice is separated by 2μm.

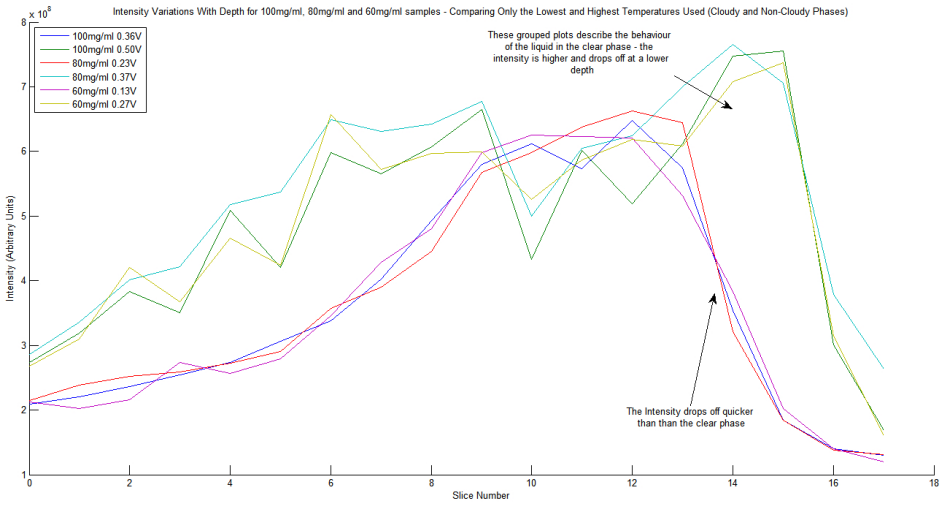

Figure 22: This image shows how the intensity varies with depth for all of the concentrations tested. The data plotted only considers the extremes in temperature that were tested and compares how the phase change effects how much light is transmitted through the samples. Each slice is separated by 2μm.

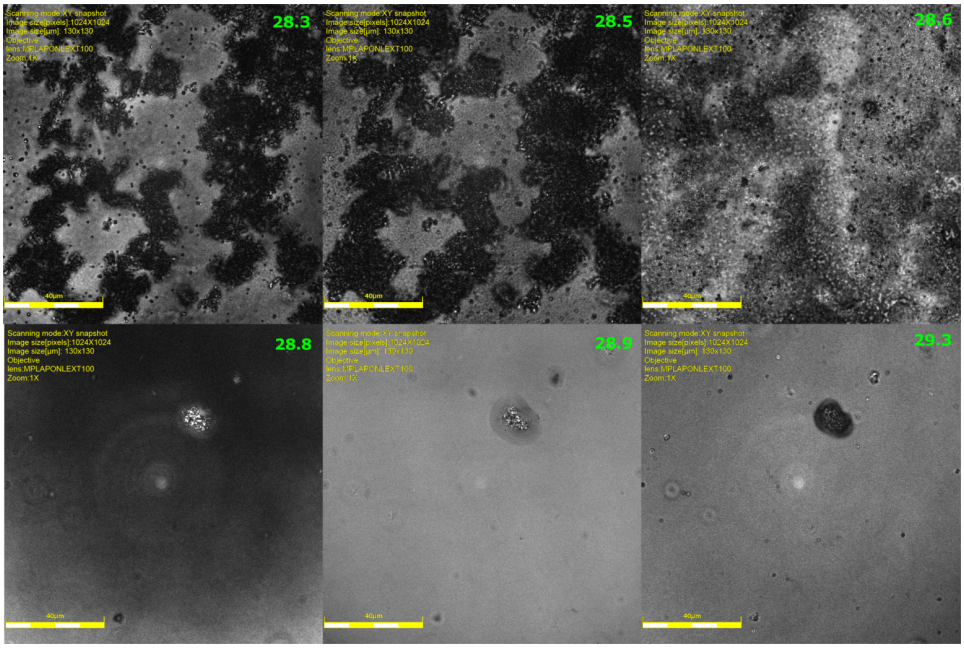

Figure 23: This image shows some of the images obtained around the phase boundary in a 100mg/ml solution on lysozyme in a 7% w/v NaCl, 0.1M pH 5.2 NaAc solution. The numbers in green represent the temperatures of the slices in °C. These images were captured using the confocal microscope using a 100x magnification lens. The phase boundary can be seen to be located in between the third and fourth slices (from left to right, top to bottom). This corresponds to temperatures of $28.6 \pm 0.3\,^{\circ}\mathrm{C}$ and $28.8 \pm 0.3\,^{\circ}\mathrm{C}$ when comparing the operating power of the Peltier heater to Figure 8.

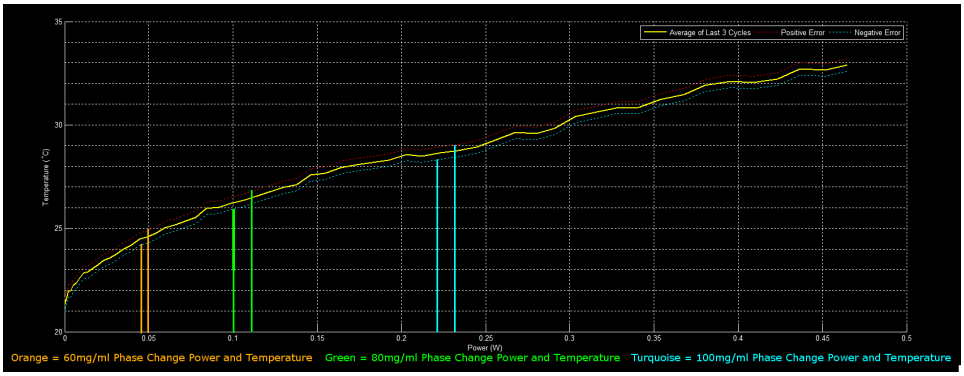

Figure 24: This image shows where the phase boundaries were observed for the 100mg, 80mg and 60mg lysozyme solutions. The phase change occurred between two power values. The lower bound of the phase change is given by the the highest power attributed to the cloudy phase (including the negative error in temperature to account for error better). The higher bound of the phase change is given by the lowest power attributed with the clear phase (including the positive error in temperature to account for error better). The difference in length of the six coloured vertical lines represent the difference between temperature over the phase change. This is plotted on Figure 25.

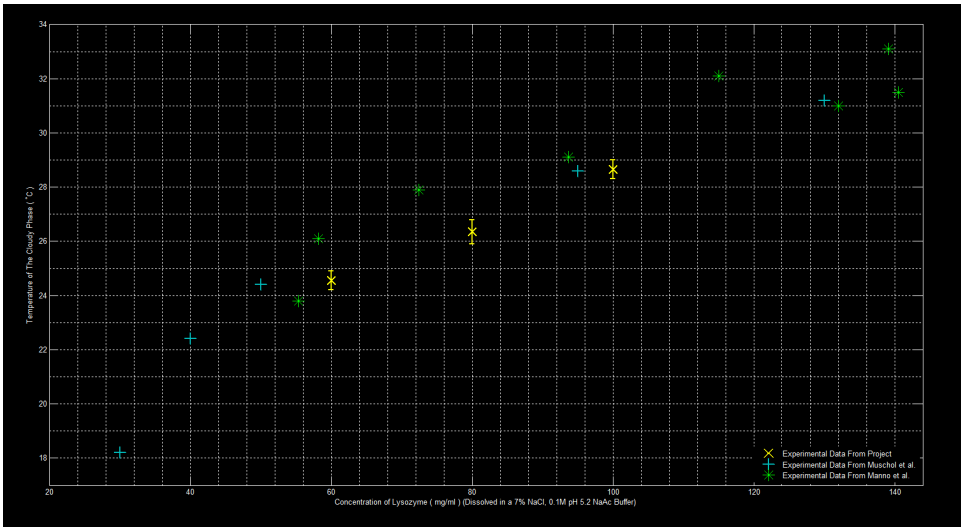

Figure 25: This image plots the phase change data gained in this experiment (Yellow). The temperature of the experimented phase boundary is the middle value of the range in temperature that the phase change occurred at (see Figure 24). The error bars are given as half of the range of temperature that the phase change occurred over. It also plots the data obtained by Muschol et al. (Turquoise) and Manno et al. (Green) [14, 15].

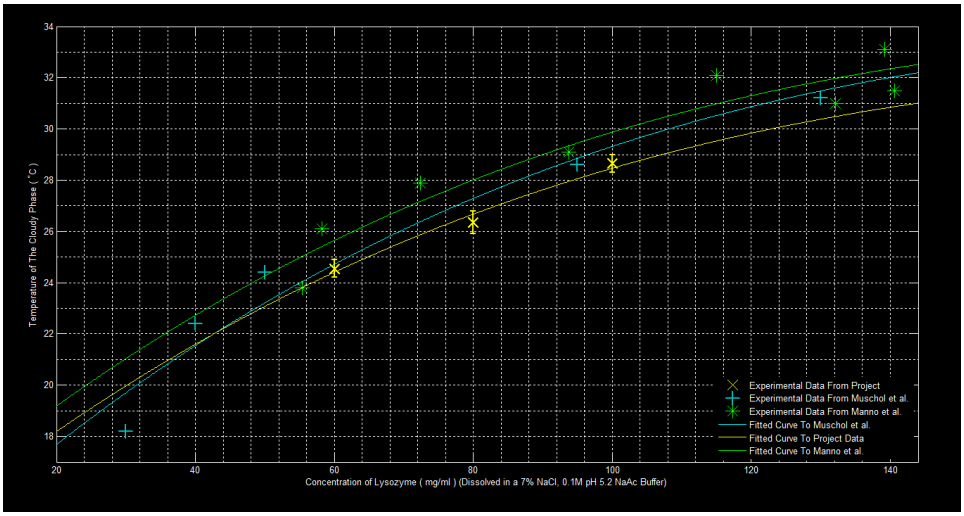

Figure 26: This image plots the same data as in Figure 25 but includes the computed fits to the experimental data sets using Equation 1 (see Section 6.2.4). The turquoise line represents the fit to Muschol's data [14], the green line represents the fit to Manno's data [15] and the yellow line represents the fit to the experimental data obtained in this project.

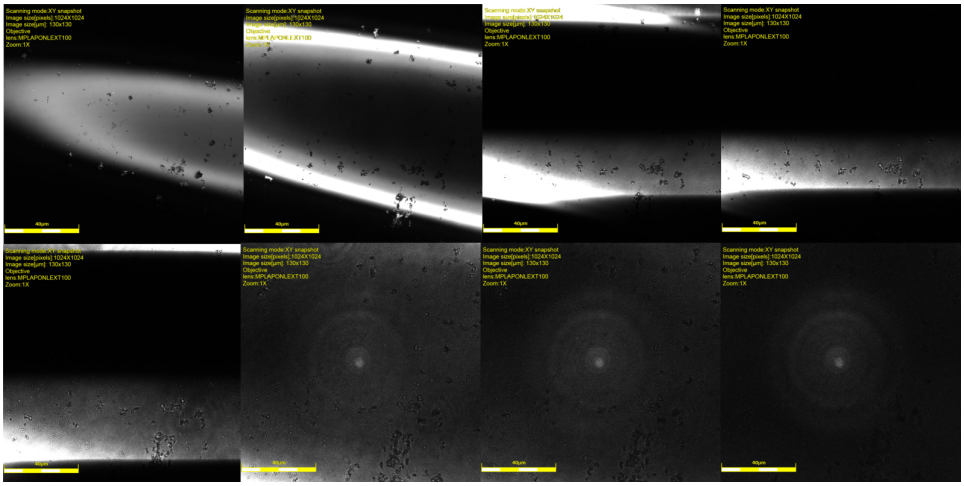

Figure 27: This image some slices of a 100mg/ml lysozyme sample in a capillary, each slice is progressively deeper into the sample. Unfortunately, the shape of the capillary lead to unwanted intensity spikes and the inability to focus on the liquid successfully as indicated by the top images. Also the capillary was too thick and gravitational effects led to the high density phase sinking (why there is no dark phase in this liquid).